PFC/RR-85-16

FIELD DERIVATIVE CONTOURS OF EFFECTIVENESS FOR FILAMENTARY CURRENT LOOPS

R.J. Thome, R.D. Pillsbury, Jr.,
J.M. Tarrh and W.R. Mann

January 1986

Plasma Fusion Center
Massachusetts Institute of Technology
Cambridge, Massachusetts 02139 USA

FIELD DERIVATIVE CONTOURS OF EFFECTIVENESS FOR FILAMENTARY CURRENT LOOPS

R.J. Thome, R.D. Pillsbury, Jr., J.M. Tarrh and W.R. Mann
Plasma Fusion Center
Massachusetts Institute of Technology
Cambridge, MA 02139

ABSTRACT

The concept of adjusting field derivatives at a collection of points to create a desired field profile has been used. However, applications have been hampered by the difficulty of obtaining closed-form expressions for the higher derivatives of the field from a loop. Algebraic manipulation computer codes have alleviated the problem and have been used to generate the derivative coefficients up to sixth order for the flux function for a circular filamentary current loop. The coefficients have been cast into a normalized form and presented in two sets of twelve charts which allow loop locations of constant effectiveness to be visualized. The charts provide contours in normalized space along which different loops will provide the same derivative coefficient per ampere turn or per ampere meter for a general point relative to the coil. An example based on the relative importance of coils in an ideal poloidal field coil set for a tokamak is also given.

INTRODUCTION

Figure 1 shows a circular current filament carrying I ampere-turns. The coil has a radius "a" and is a distance "d" above the z = 0 plane in a system where the field point of interest is at $(R_0,0)$. The vector potential or field components at $(R_0,0)$ can be related to the flux function $\psi = 2\pi R_0 A$ where ψ is the total flux through a loop of radius R_0 in the z = 0 plane and A is the azimuthally directed vector potential (eg See [1]). This allows the fields produced by a set of filaments with known currents to be analyzed by superposition. The inverse problem of synthesizing a desired field shape by determining the required currents in a set of coils which are only partially constrained in number and location is more difficult.

If the flux function in the vicinity of a point due to one set of sources is known, then the field derivatives at the point are known in principle. Furthermore, the same field distribution in the vicinity of the point may be approximated by a second set of sources if the second set is adjusted in location or strength such that it matches the magnitudes of a sufficient number of the desired field derivatives. For an off-axis point such as $(R_0,0)$, it is sufficient to know and match a number of the derivatives of the r and z field components with respect to "r" only (see Appendix A).

In this report, plots with contours of constant effectiveness show locations in the rz-plane at which coils will create the same magnitude of vertical or radial field, or their derivatives up to fifth order. Effectiveness coefficients are normalized on an ampere-turn basis to show the changes required in coil current to achieve the same field component or nth

order field derivative with different coil locations. A second set of charts is given in which the field and derivative coefficients are normalized on an ampere meter basis, since this is often of interest in superconducting coils. The charts are general and there is no restriction on location of the point of interest relative to the coil.

As an example, this paper also has results from a study which uses the contours to show that, if a high degree of plasma shaping is required, a PF coil or coils near the midplane on the inboard side of a tokamak should be allowed to have a current independent of the central ohmic heating solenoid stack or, equivalently, the midsection of the central solenoid should not be constrained to have the same current as the balance of the stack. The concept of matching field derivatives has been used as the basis for a tokamak poloidal field coil system evaluation code [2].

CONTOURS OF CONSTANT EFFECTIVENESS

The normalized flux function at $(R_0,0)$ due to the filament at (a,d) in real space or (ρ,η) in normalized space is given by:

$$\frac{\psi}{R_0 \mu_0 I} = 2\pi \frac{\rho^{1/2}}{k} [(1 - k^2/2)K - E] \qquad (1)$$

where:

μ_0 = $4\pi \times 10^{-7}$ = permeability of free space

I = coil current

k^2 = $4\rho[(1 + \rho)^2 + \eta^2]^{-1}$

ρ = a/R_0 = normalized coil radius

η = d/R_0 = normalized coil distance to $z = 0$

K,E = complete elliptic integrals (1st, 2nd)

The first and second derivatives of this expression can be done in a straightforward fashion. Higher order derivatives become difficult by hand, but can be done with a computer-based algebraic manipulation code (e.g. - MACSYMA [3]). This was done for derivatives up to fifth order (i.e., n = 6) with results too lengthy to reproduce here. However, the derivatives may be shown to have the following normalized form.

$$\frac{\partial^{n-1} B_k}{\partial r^{n-1}} = \frac{\mu_o I}{R_o^n} \; p_{nk} \qquad (2)$$

where:

k = r,z

n = 1,2,3..

p_{oo} = Eq (1) for n = 0

p_{nk} = $p_{nk}(\rho,n)$ = normalized field or derivative per ampere turn

Coil locations with the same value of p_{nk} will produce the same flux function, vertical field, or its derivative (depending on n) at (1,0) per ampere-turn in the coil. Contours in the rz plane along which these functions have the same value will be defined as contours of constant effectiveness for the corresponding derivative. The contour plots for the normalized vertical field, normalized radial field and the higher order derivatives, are given in Figs. 2-13. Solid lines are positive contours in that a positive current as defined in Fig. 1 will produce a positive function, p_{nk} in (2), whereas dashed contours are negative in that a positive current produces a negative function in (2).

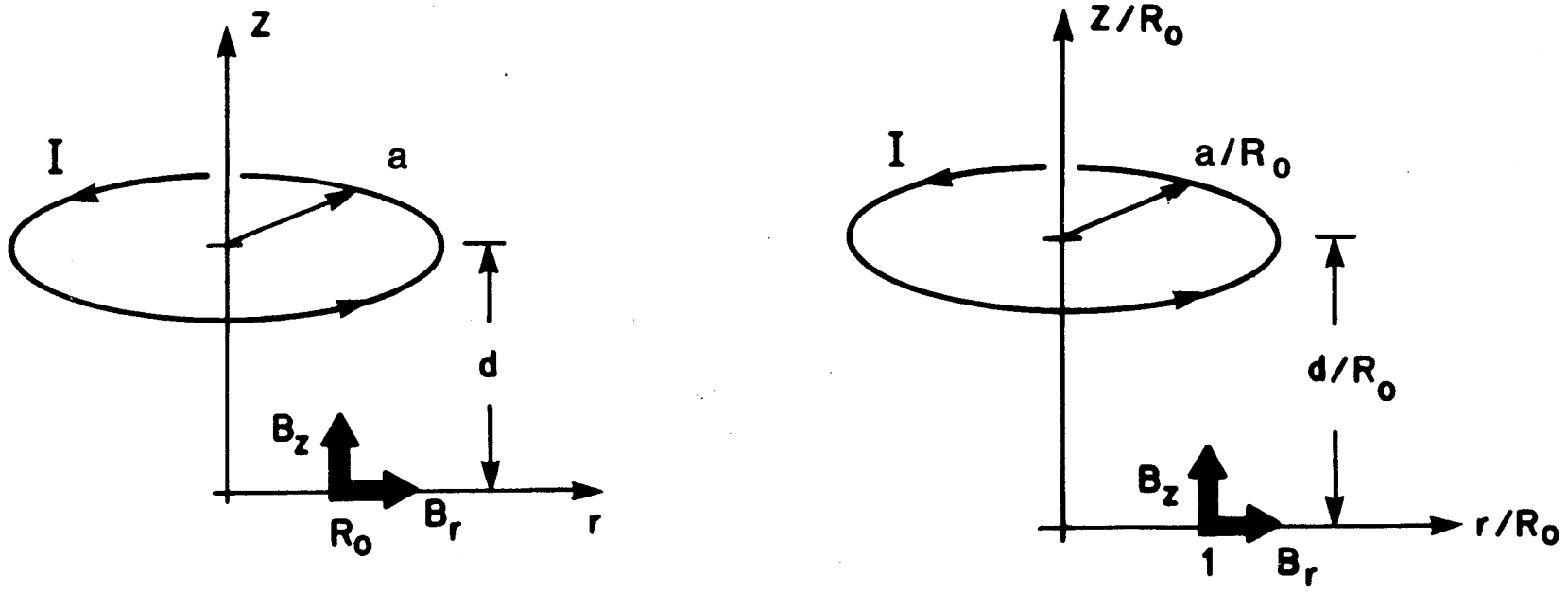

Fig. 1 - Current Filament Producing Field Components and Field Derivatives at the point $(R_o,0)$ in Real Space or (1,0) in Normalized Space

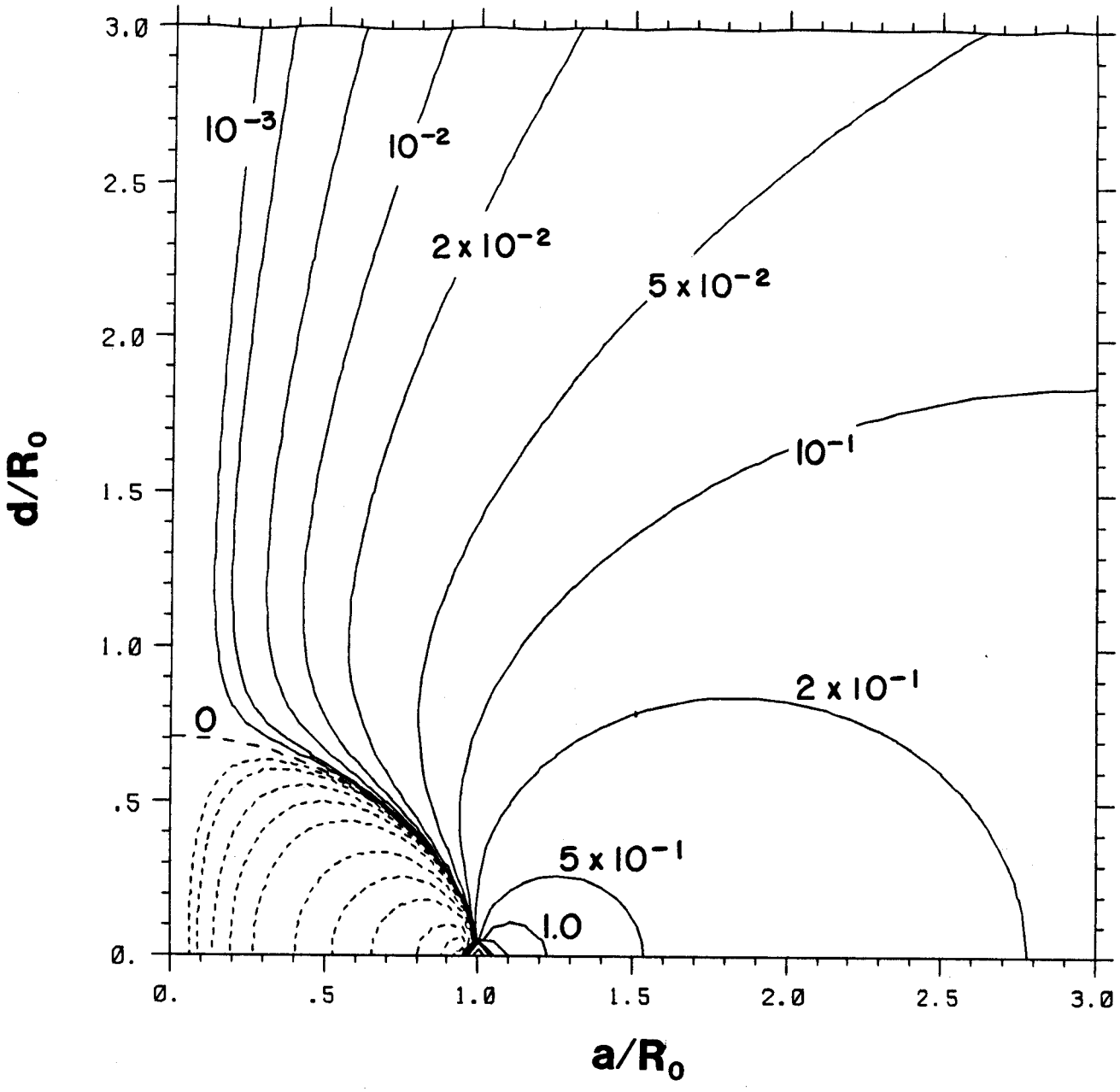

Fig. 2 - Normalized Contours of B_z per ampere turn

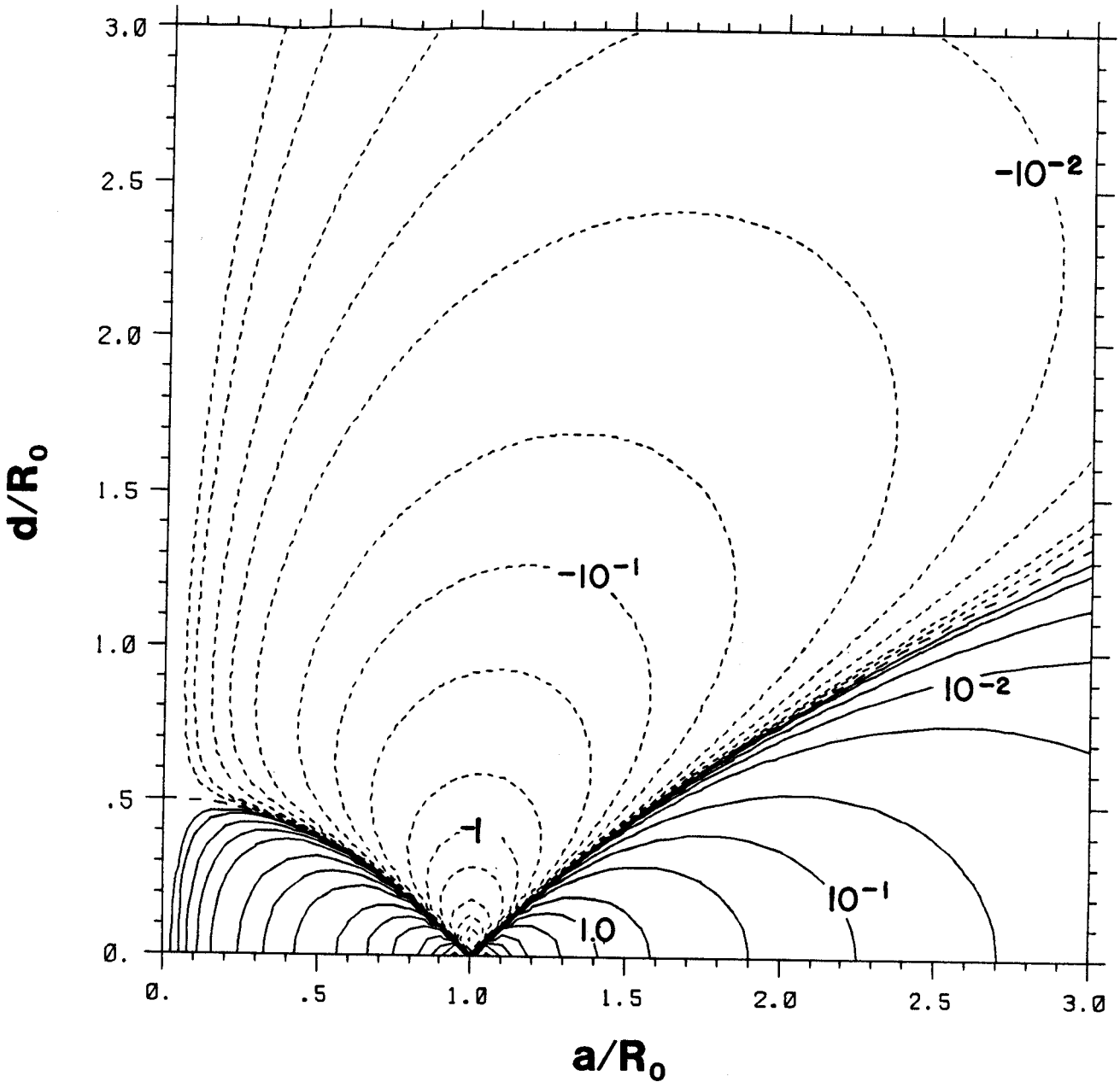

Fig. 3 - Normalized Contours of first derivative of B_z per ampere turn

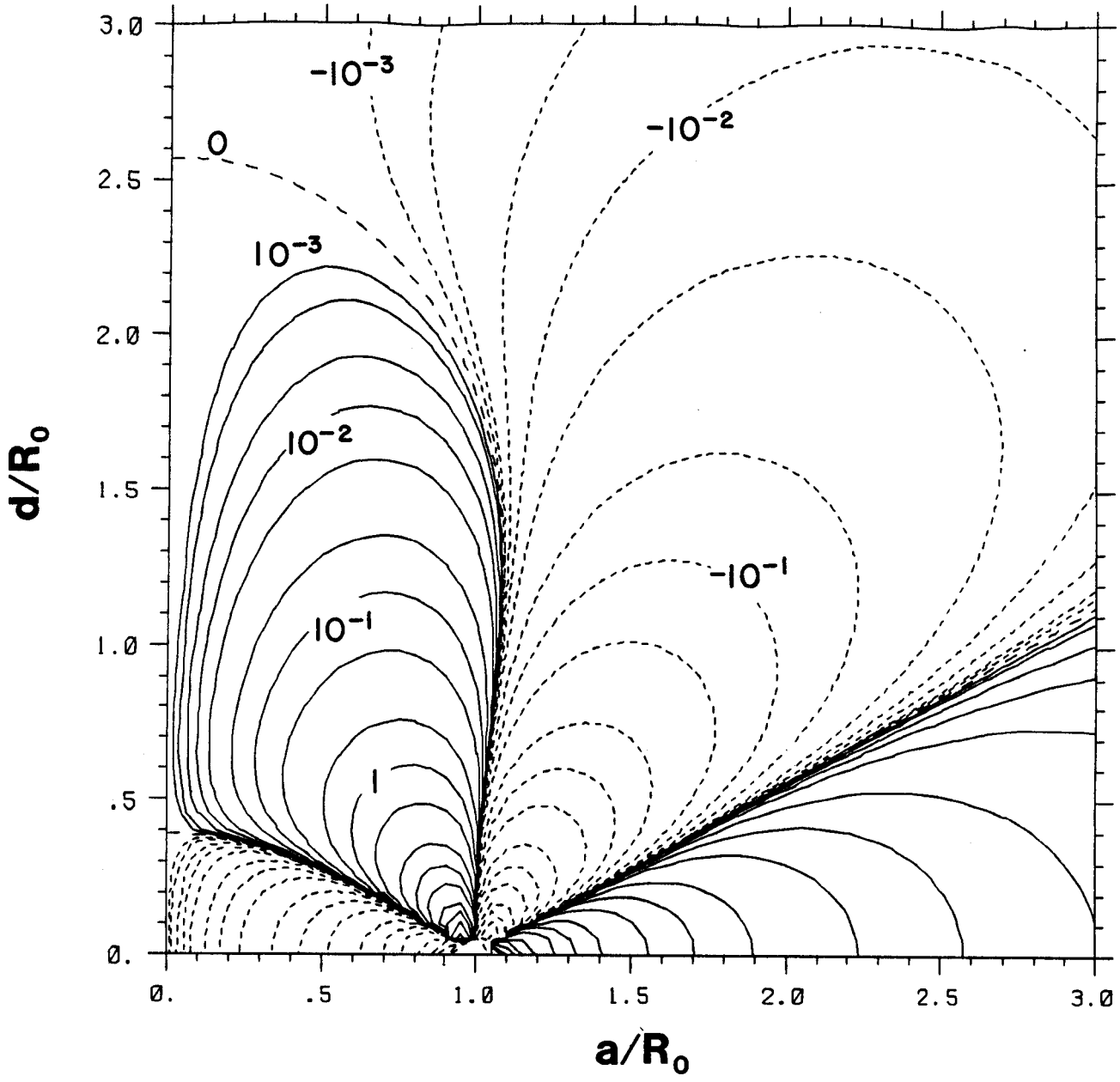

Fig. 4 - Normalized Contours of second derivative of B_z per ampere turn

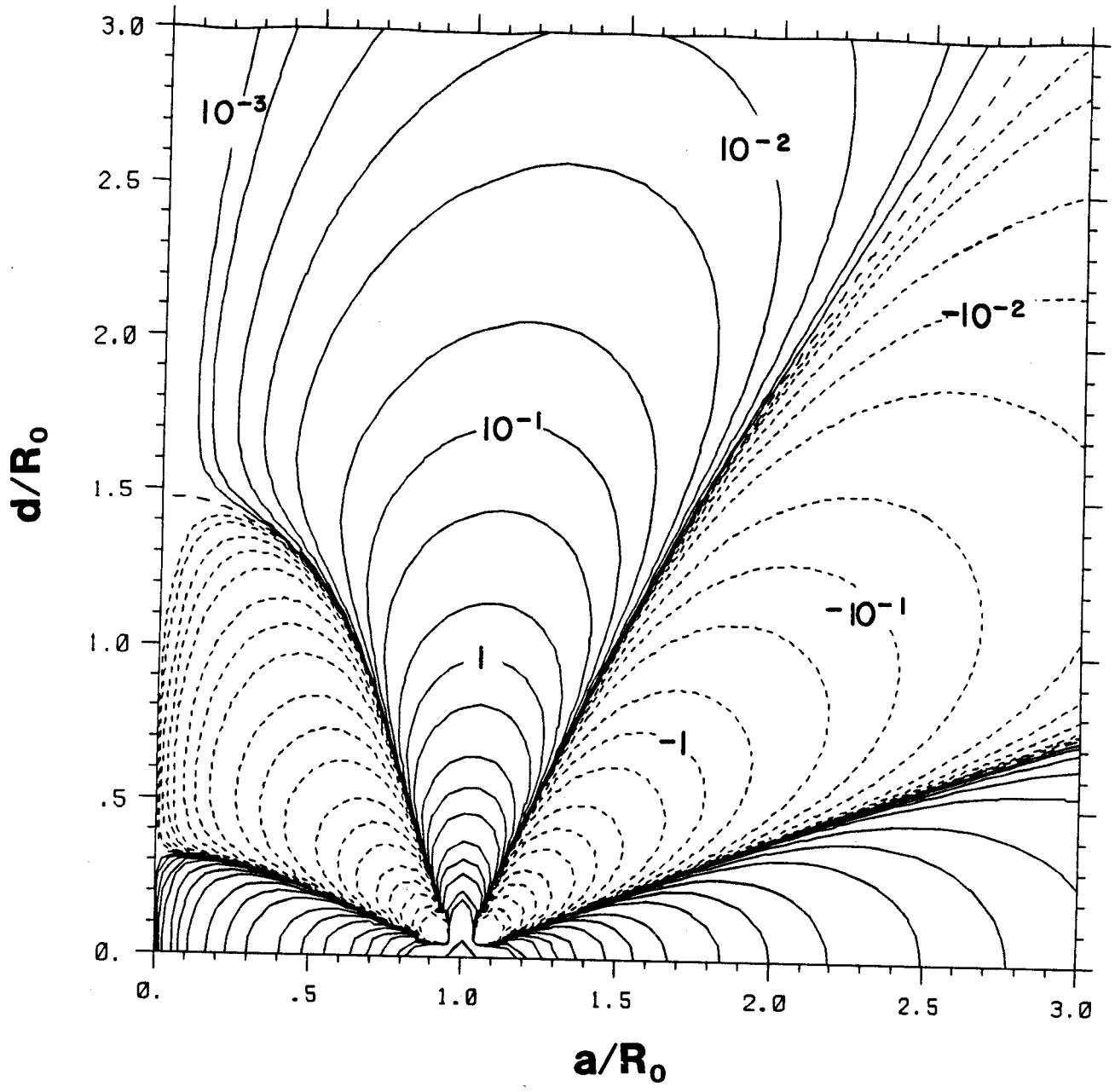

Fig. 5 - Normalized Contours of third derivative of B_z per ampere turn

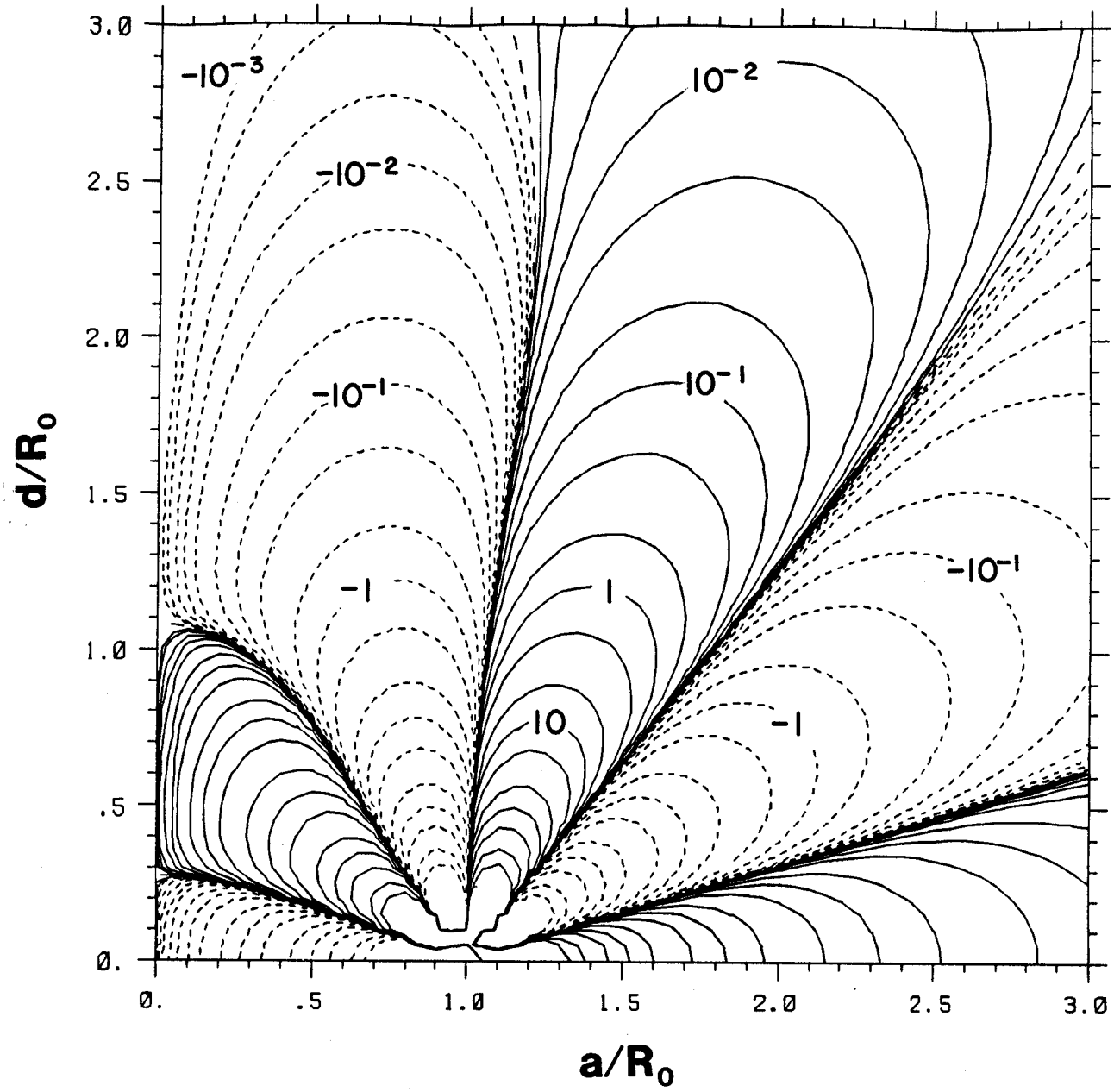

Fig. 6 - Normalized Contours of fourth derivative of B_z per ampere turn

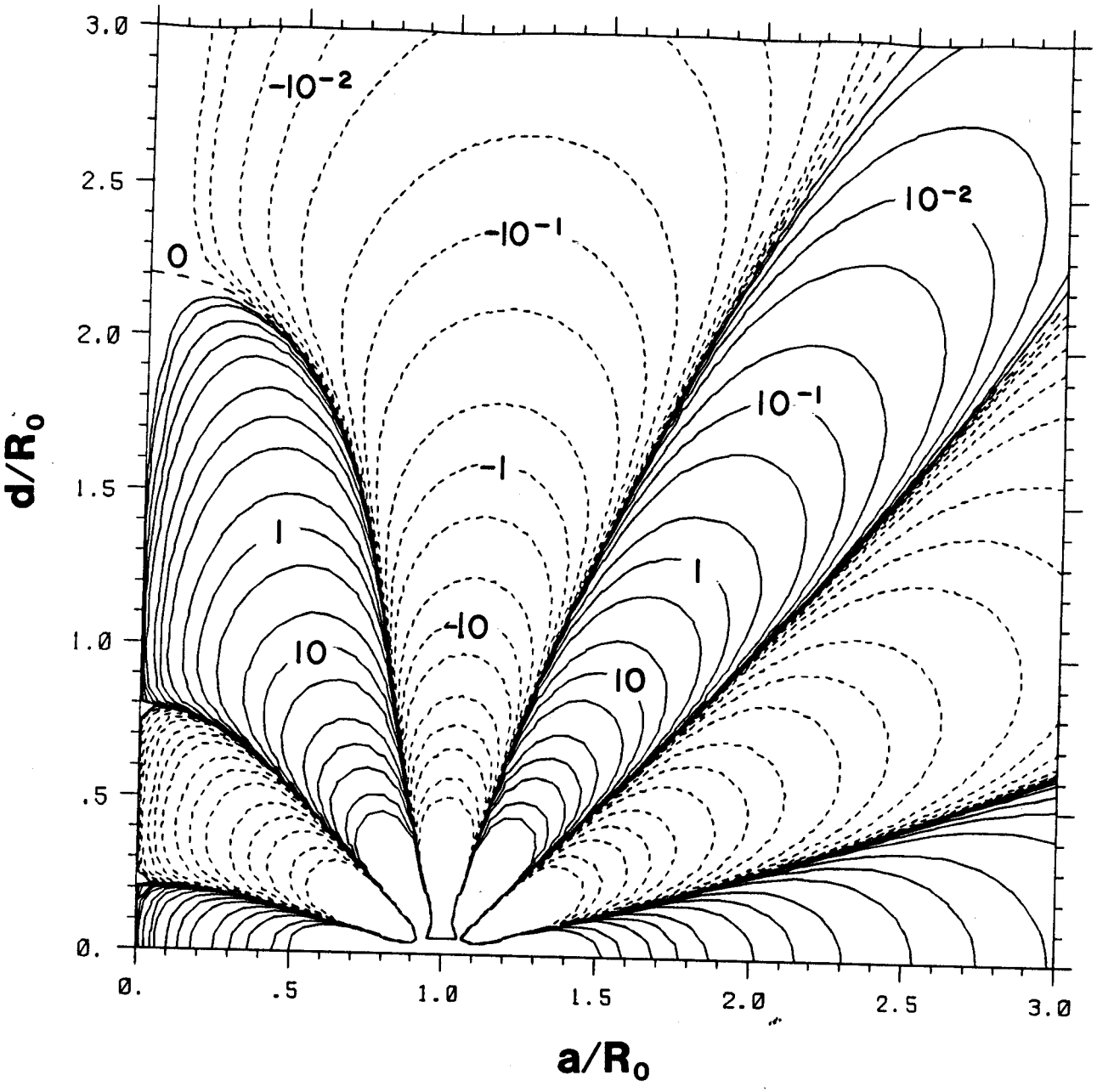

Fig. 7 - Normalized Contours of fifth derivative of B_z per ampere turn

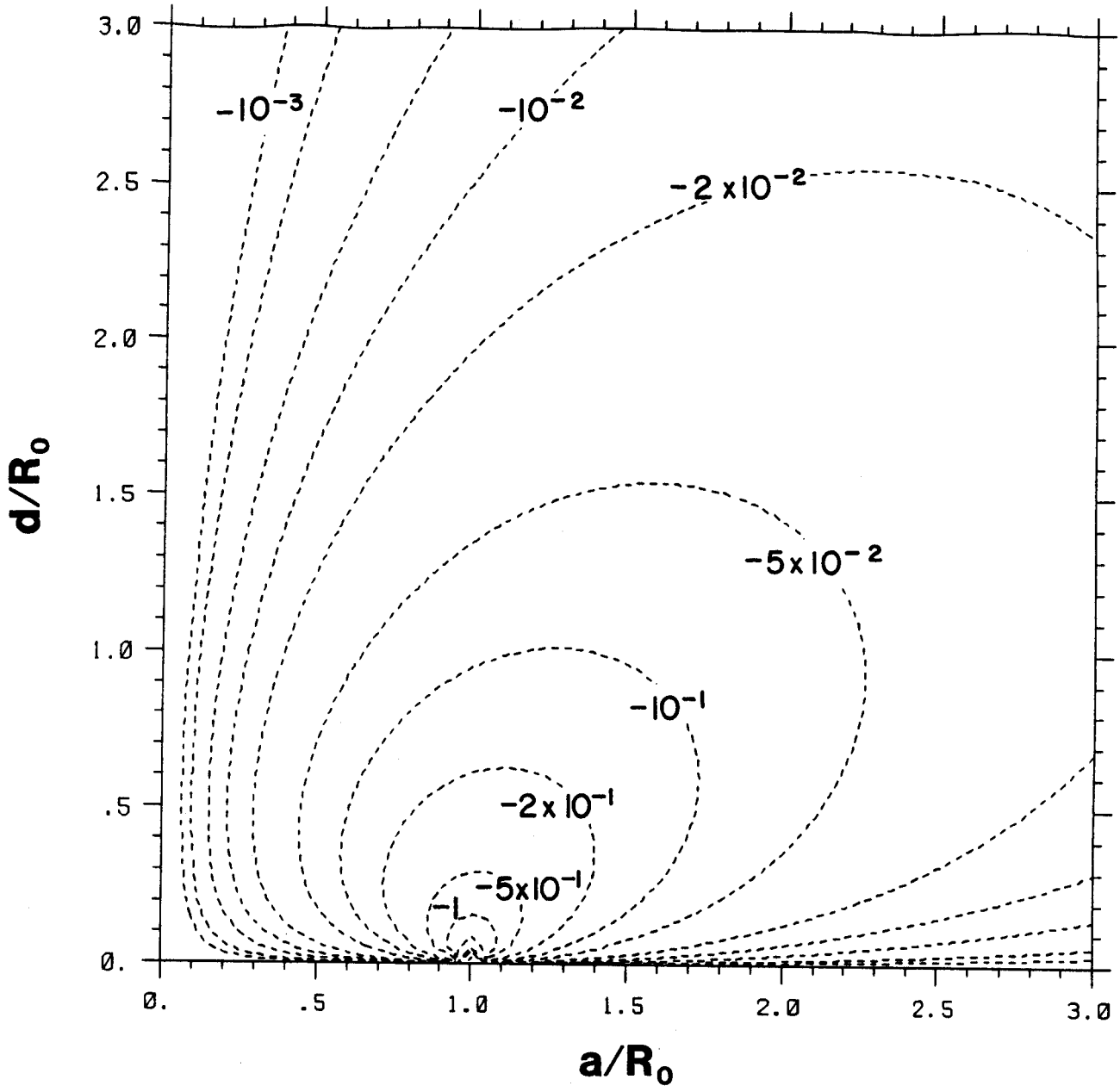

Fig. 8 - Normalized Contours of B_r per ampere turn

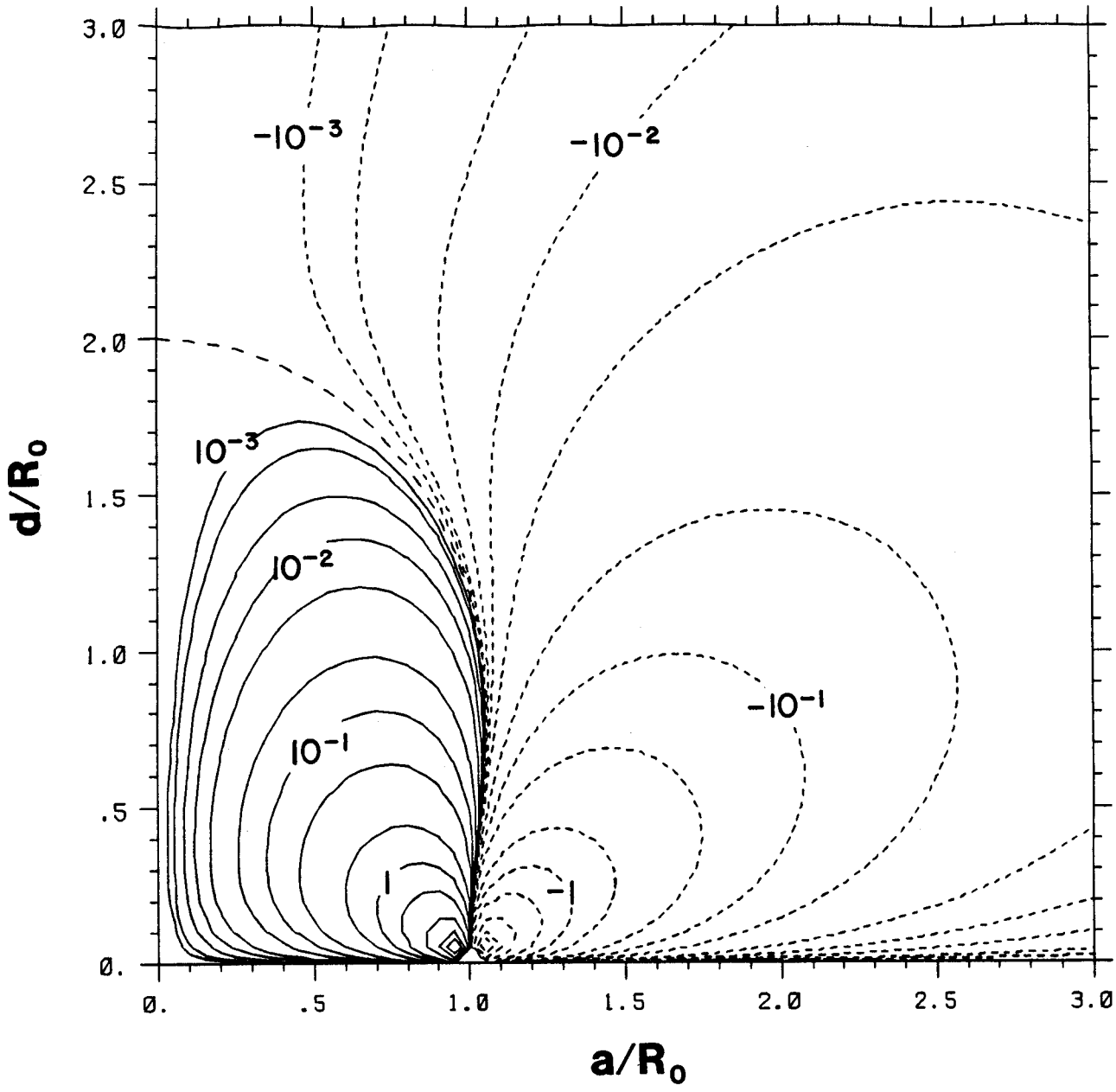

Fig. 9 - Normalized Contours of first derivative of B_r per ampere turn

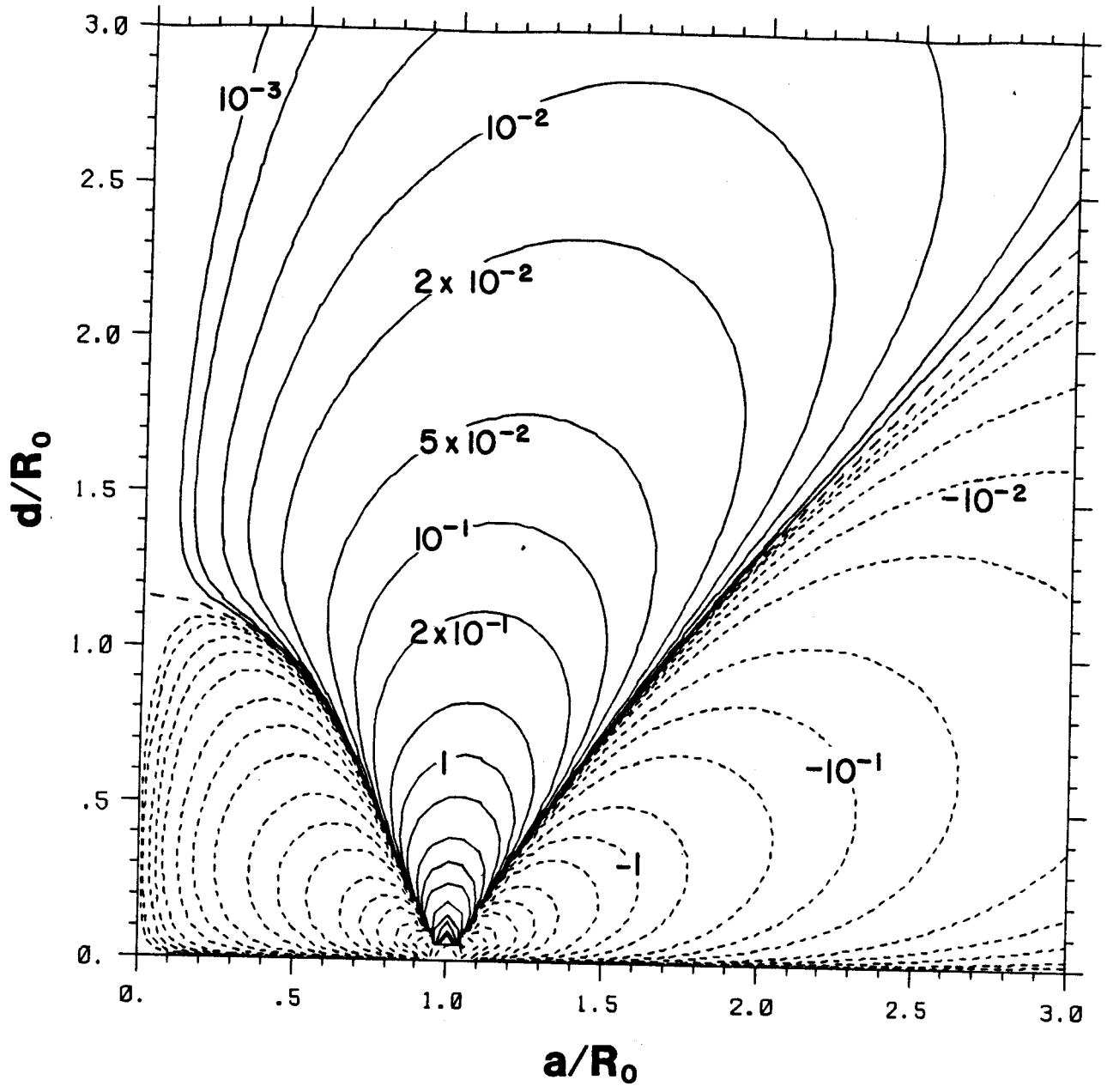

Fig. 10 - Normalized Contours of second derivative of B_r per ampere turn

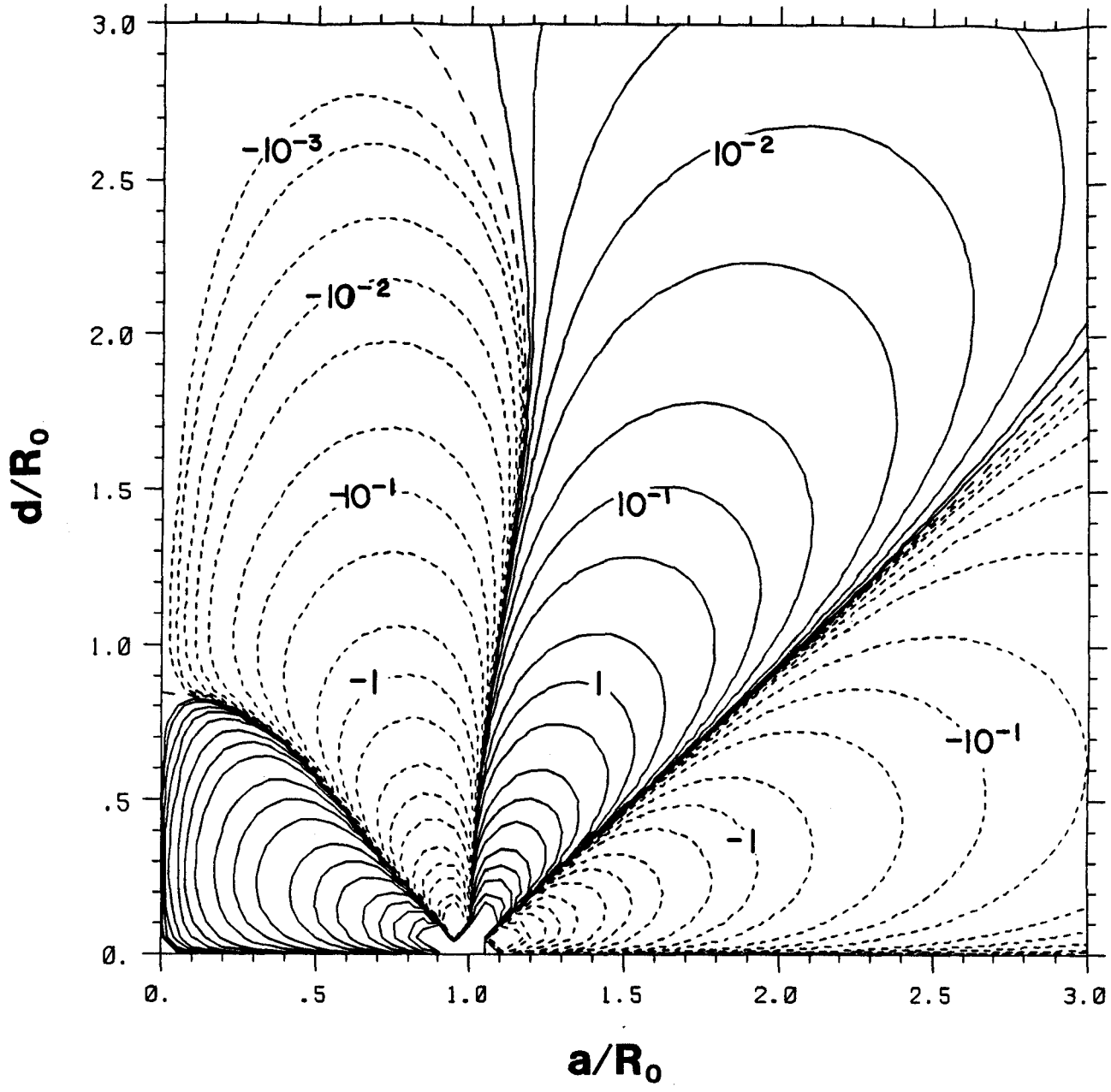

Fig. 11 - Normalized Contours of third derivative of B_r per ampere turn

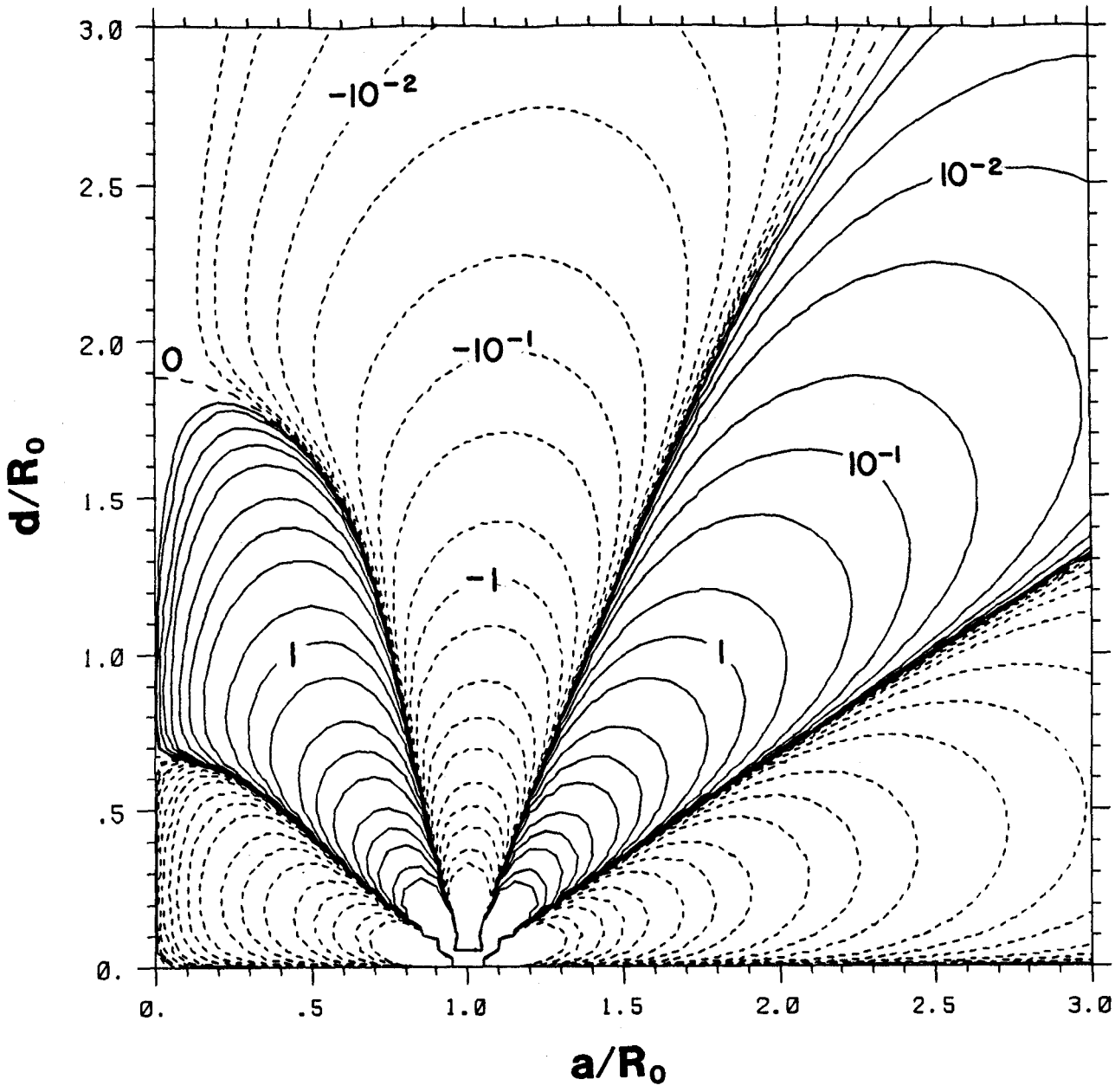

Fig. 12 - Normalized Contours of fourth derivative of B_r per ampere turn

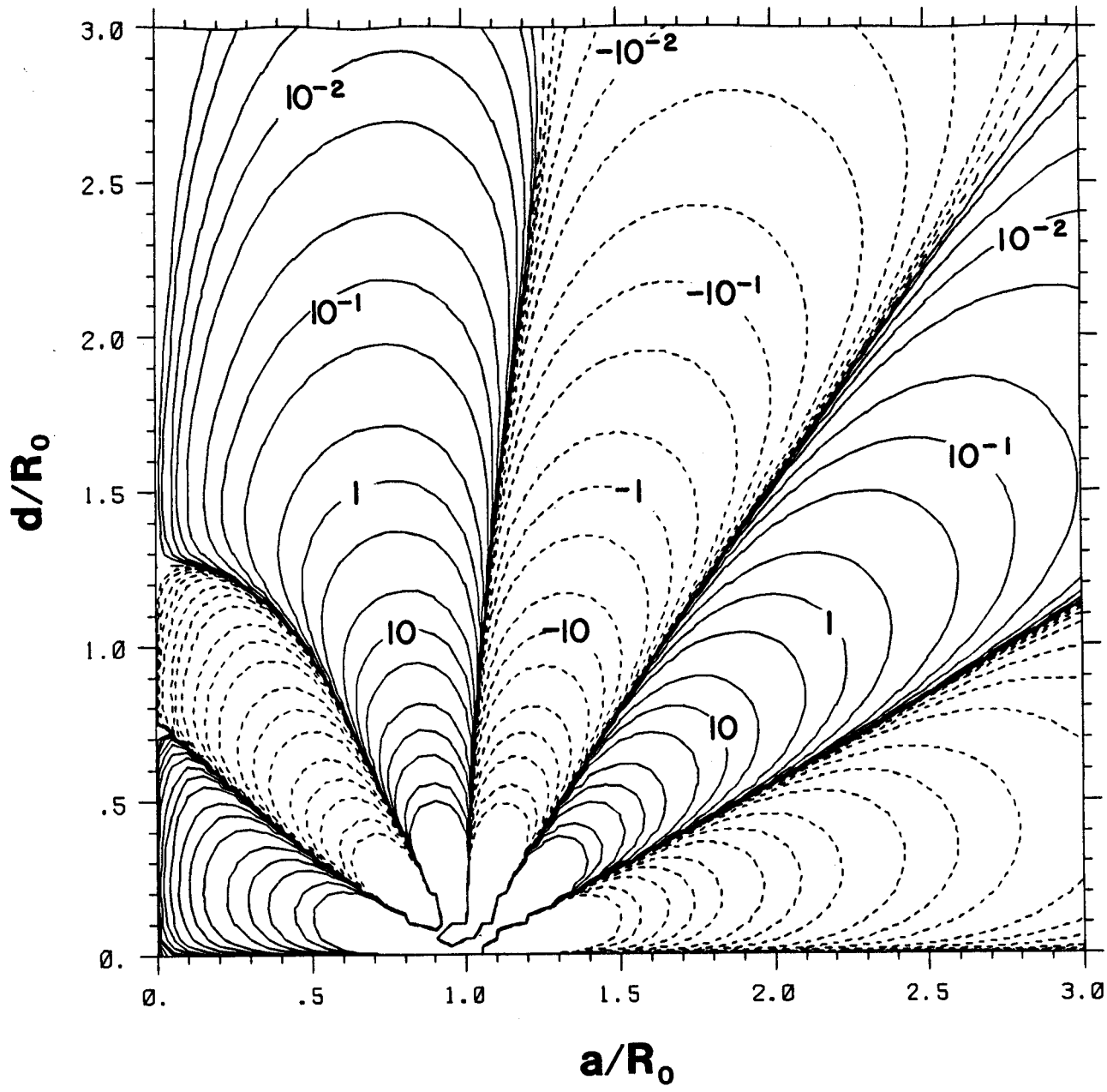

Fig. 13 - Normalized Contours of fifth derivative of B_r per ampere turn

The contours show the rapid decrease in effectiveness with distance from the point (1,0), and also indicate that the derivatives for n = 1,2,3.. have 1,2,3.. lines, respectively, along which a coil with $n > 0$ can be placed and have no contribution to that particular field derivative at (1,0). This also means that a coil located on a zero effectiveness line can contribute to other derivatives while being decoupled from the production of that particular derivative. However, contour values vary rapidly from positive to negative in the vicinity of these zero lines so that a small change in location near such a line will cause substantial changes in the current distribution among coils in the production of that particular derivative requirement. This will be more severe as the number of coils become smaller and the higher-order derivative requirements become significant (e.g. - in a tokamak poloidal field coil set for highly shaped plasmas).

These contours relate coil location and ampere-turn requirement to the magnitude of the field derivative needed. Similar plots were also generated on the basis of the ampere-meter requirement since this is often a better indicator of coil cost. These charts are also general and are given in Figs. 14 to 25. In this case the contour functions are q_{nk} defined by:

$$\frac{\partial^{n-1} B_k}{\partial r^{n-1}} = \frac{\mu_o (A \cdot m)}{R_o^{n+1}} \; q_{nk} \qquad (3)$$

where:

$A \cdot m$ = ampere meters in coil

$$q_{nk} = \frac{1}{2\pi} \left(\frac{R_o}{a}\right) P_{nk} = q_{nk}(\rho, n)$$

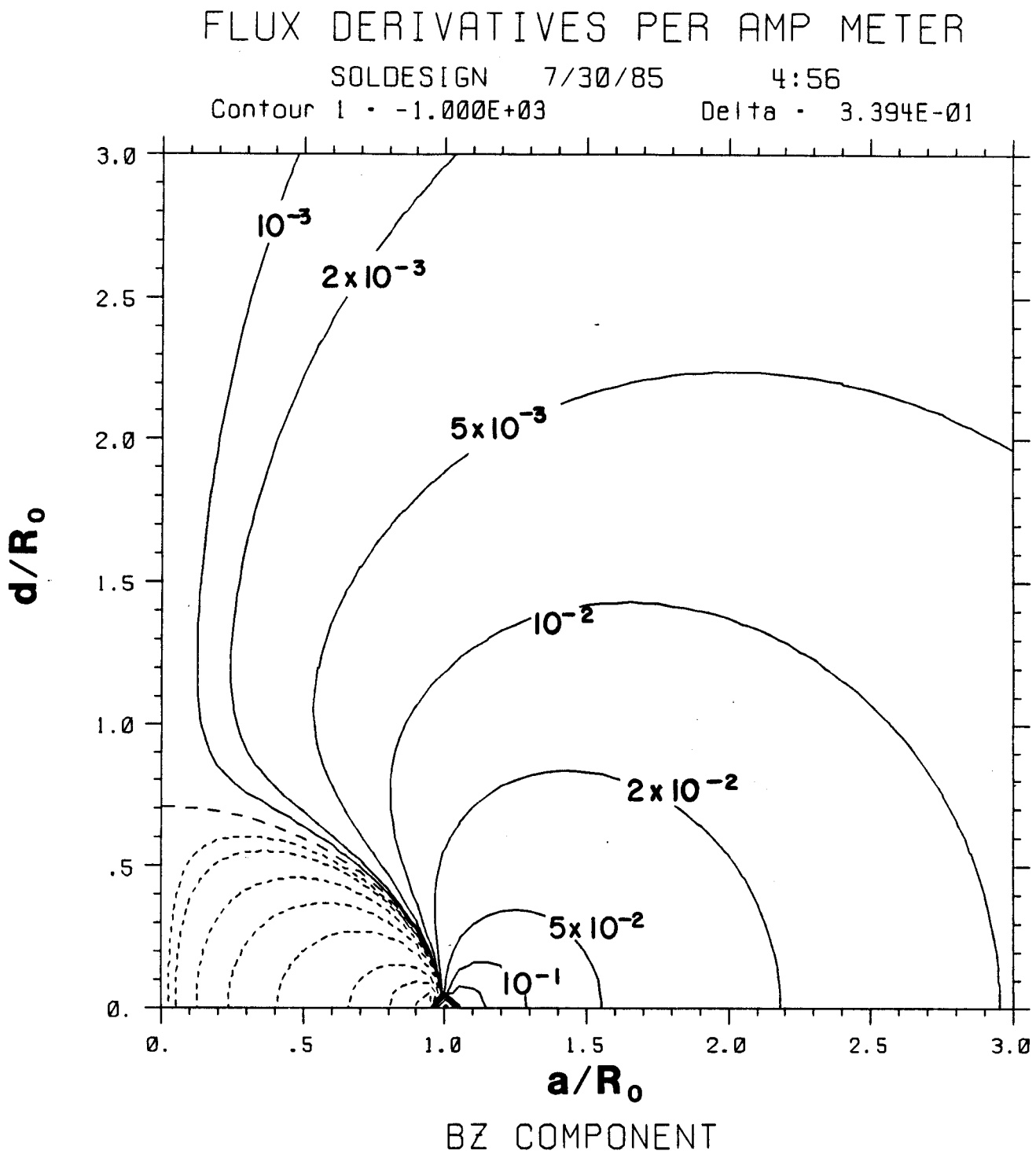

Fig. 14 - Normalized Contours of B_z per ampere meter

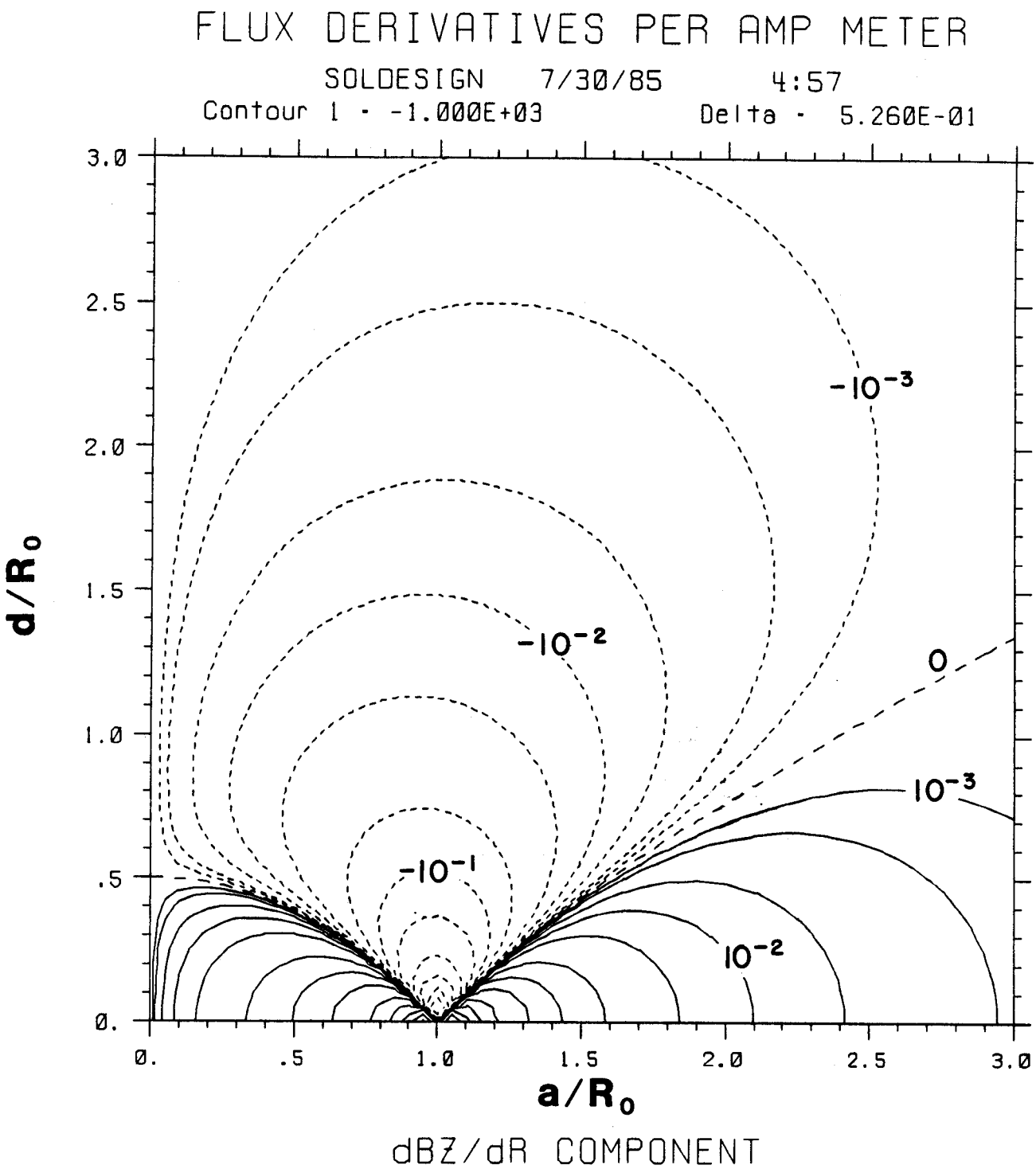

Fig. 15 - Normalized Contours of first derivative of B_z per ampere meter

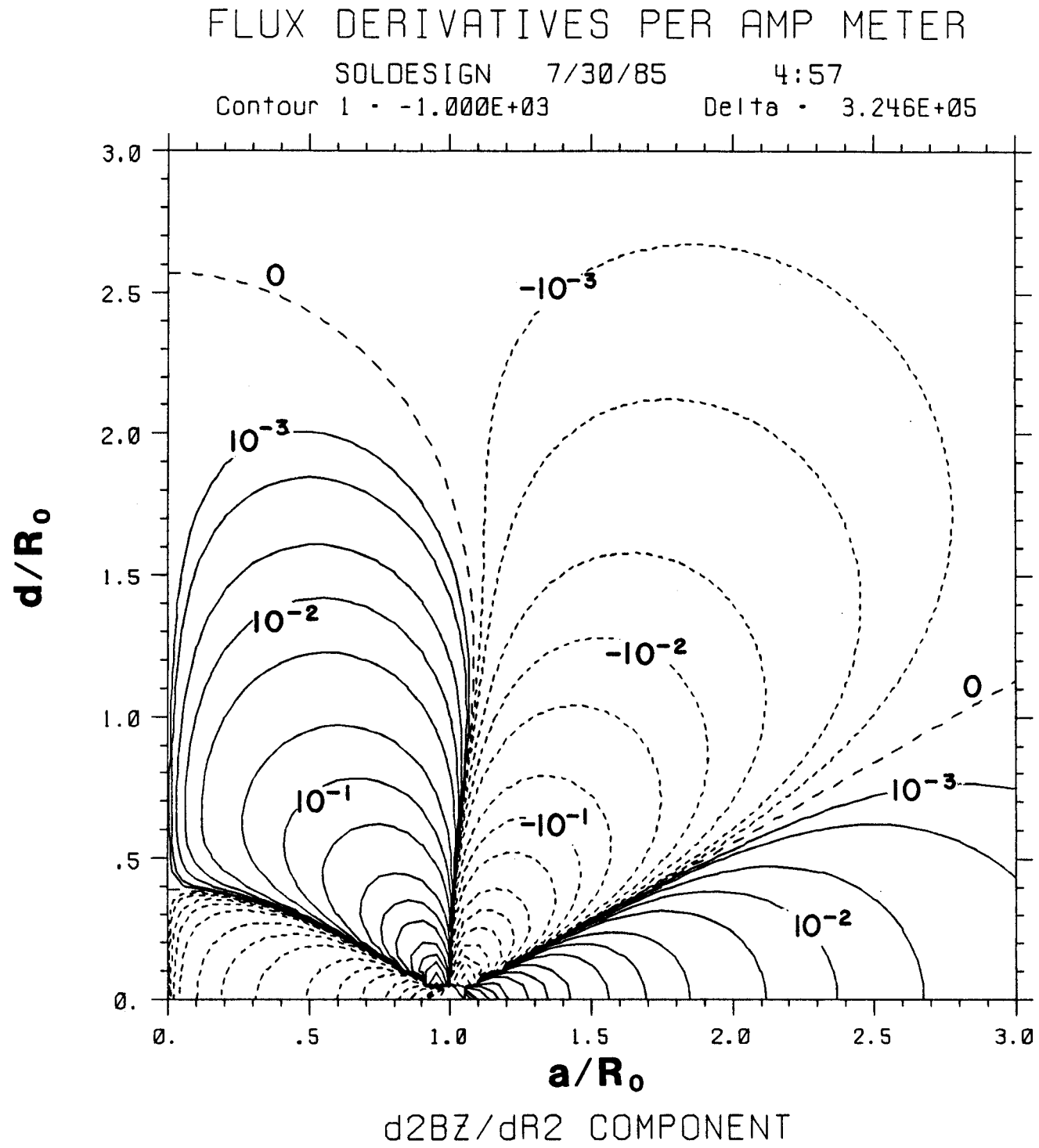

Fig. 16 - Normalized Contours of second derivative of B_z per ampere meter

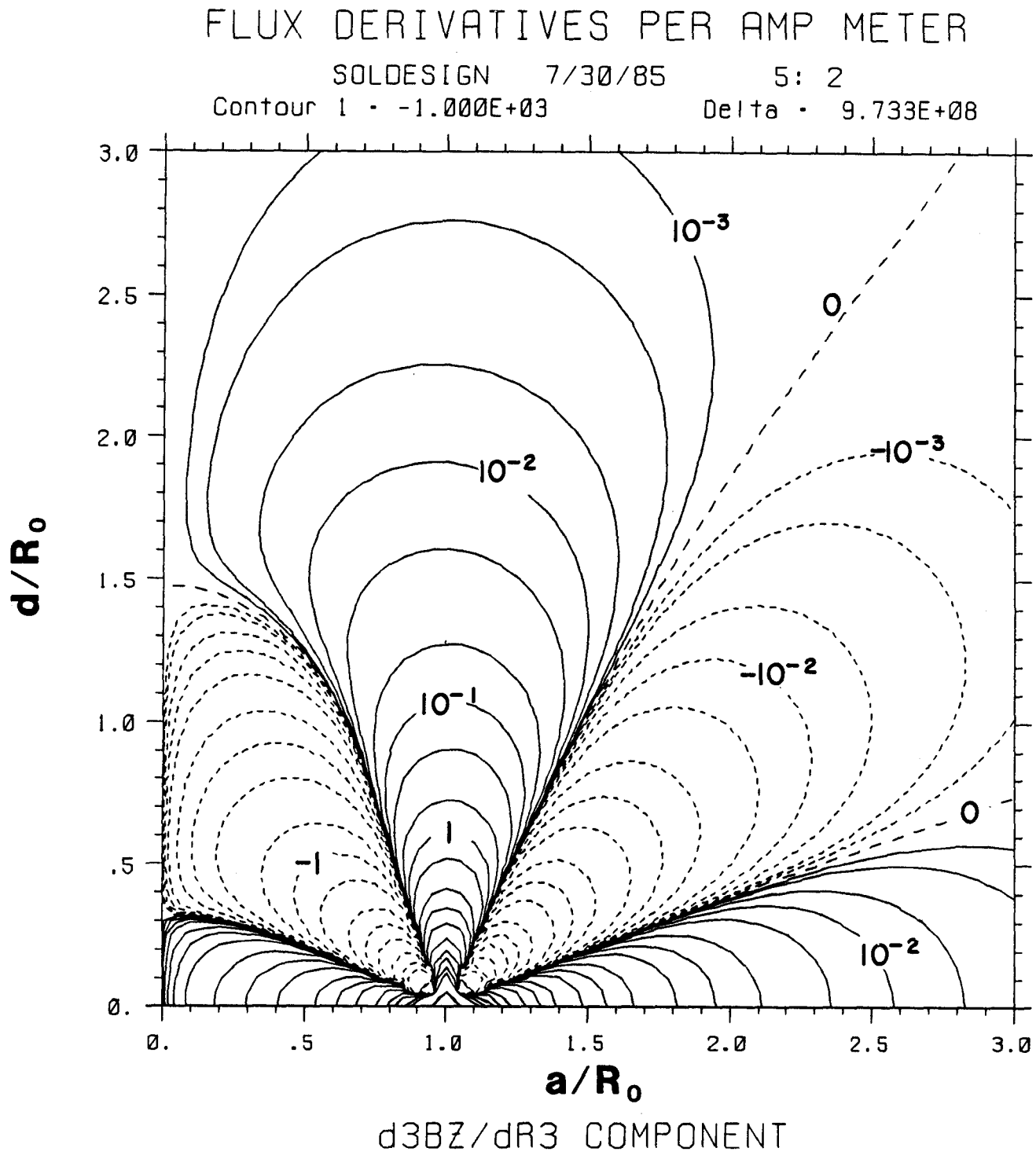

Fig. 17 - Normalized Contours of third derivative of B_z per ampere meter

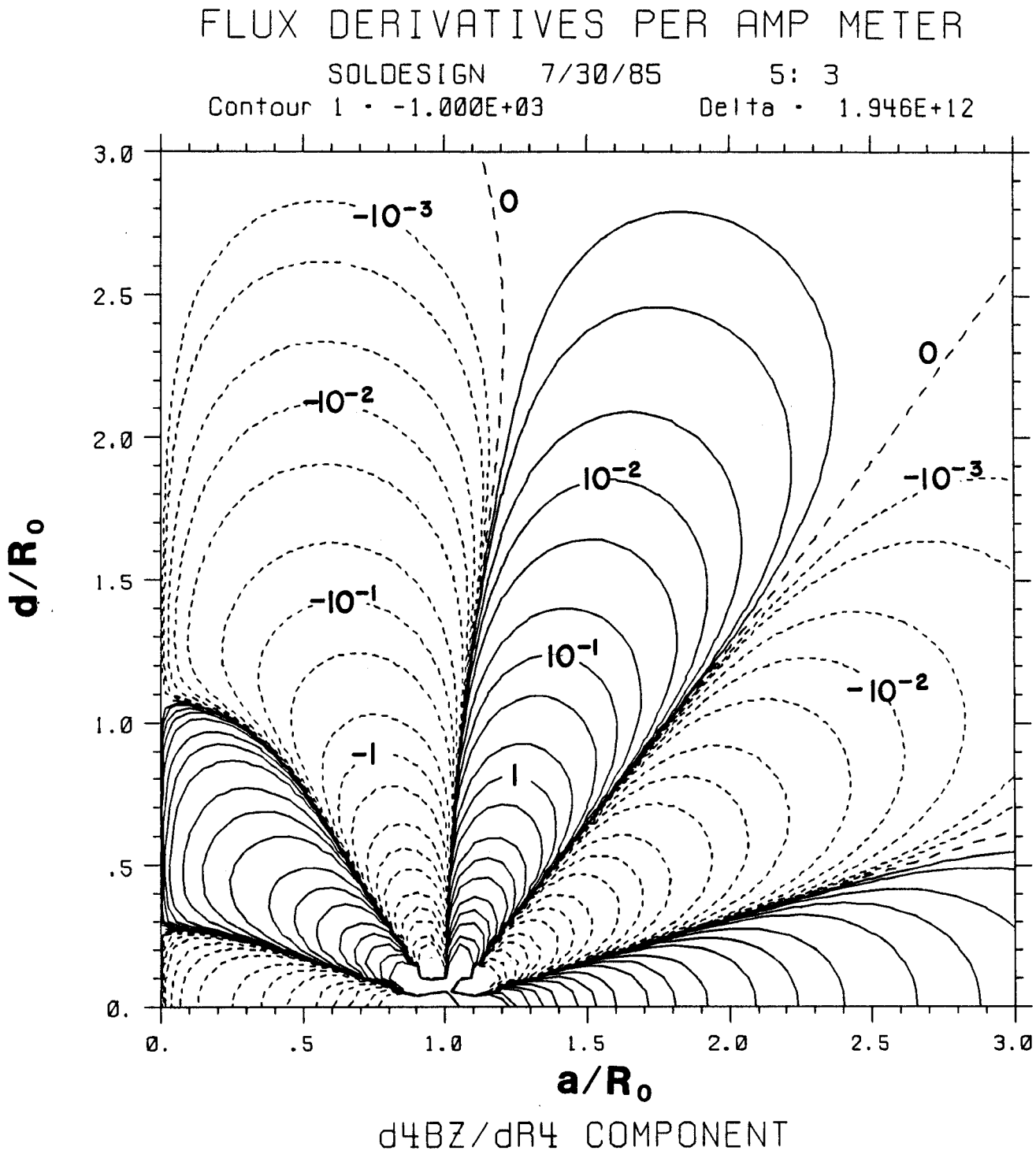

Fig. 18 - Normalized Contours of fourth derivative of B_z per ampere meter

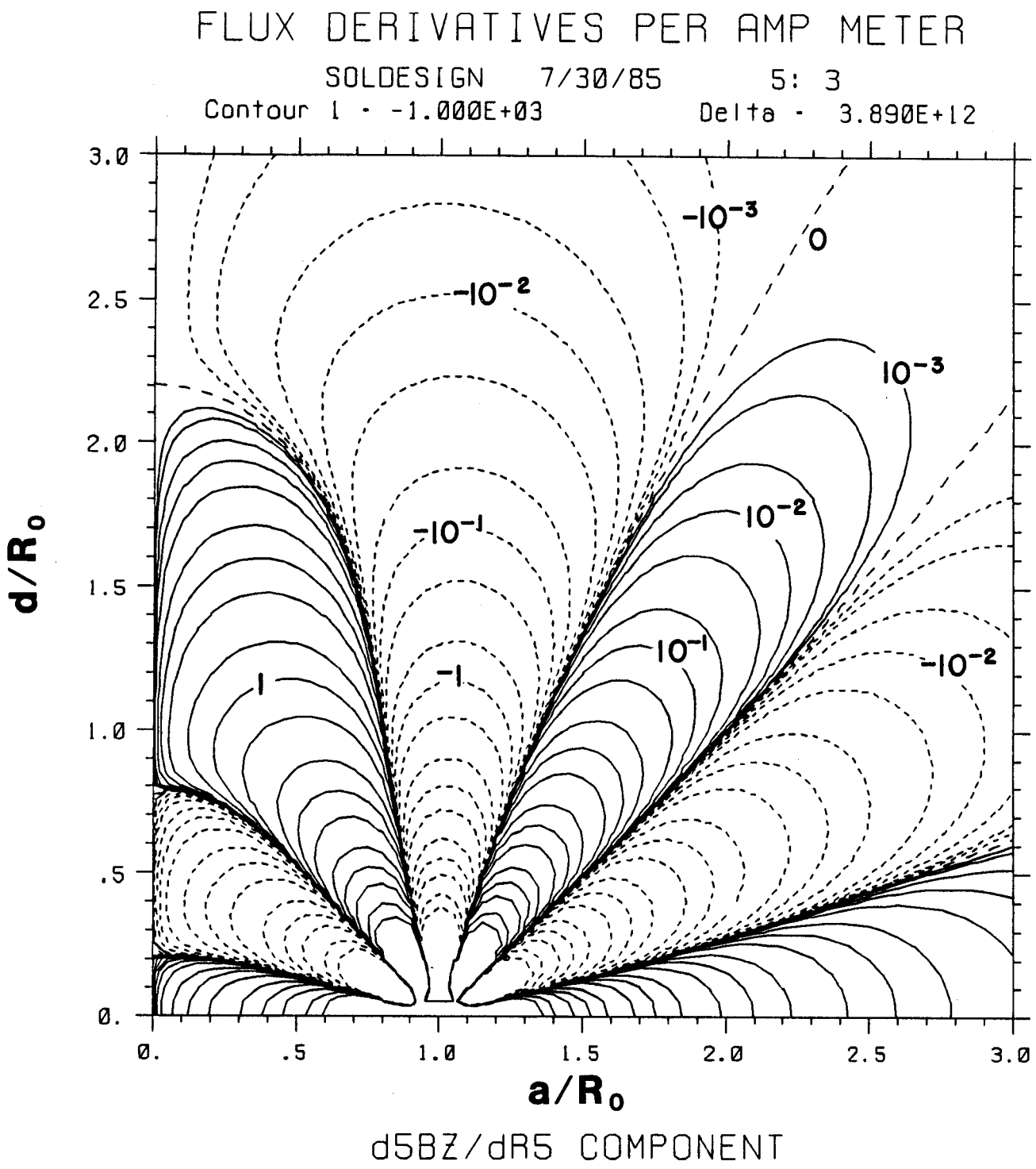

Fig. 19 - Normalized Contours of fifth derivative of B_z per ampere meter

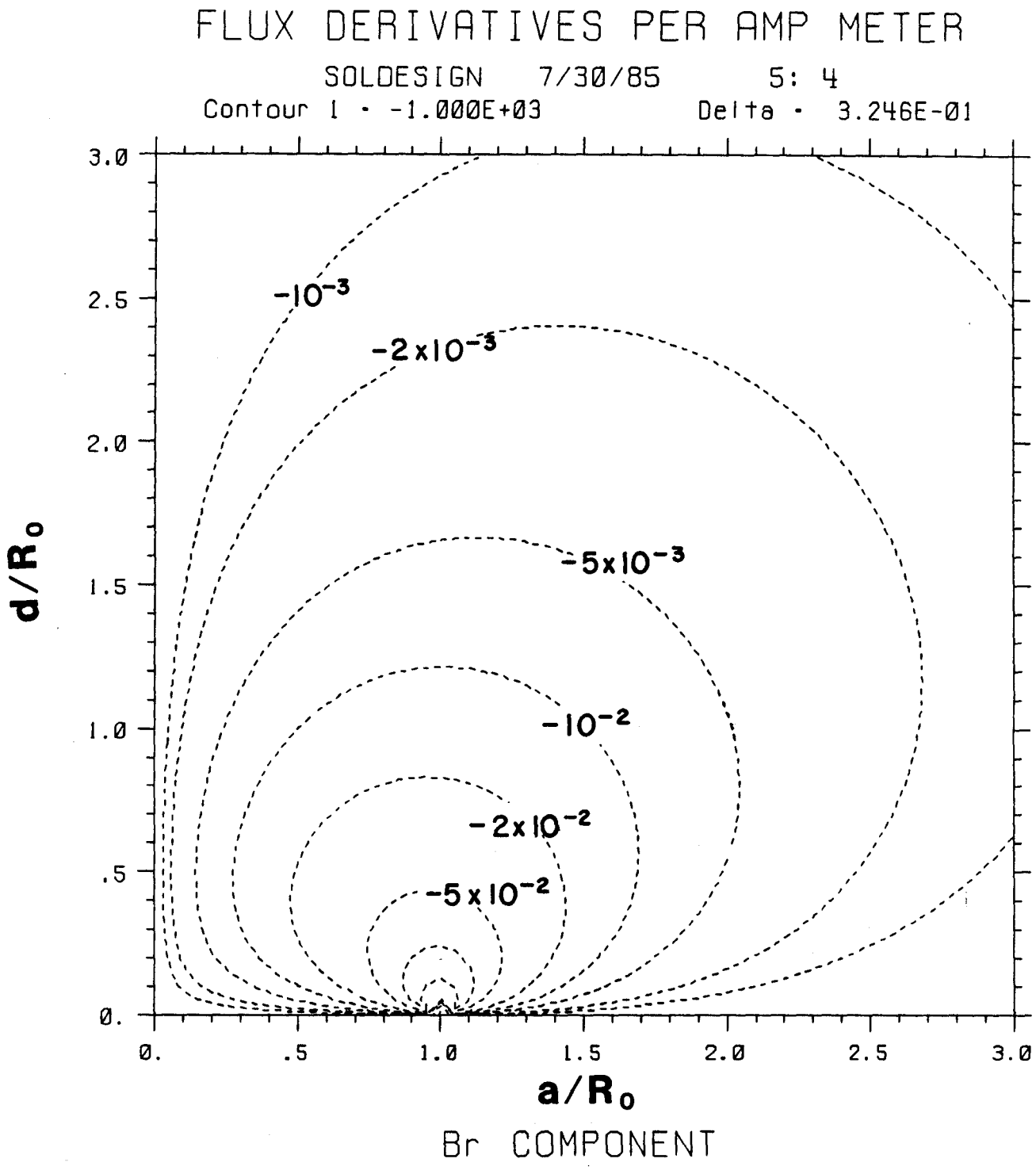

Fig. 20 - Normalized Contours of B_r per ampere meter

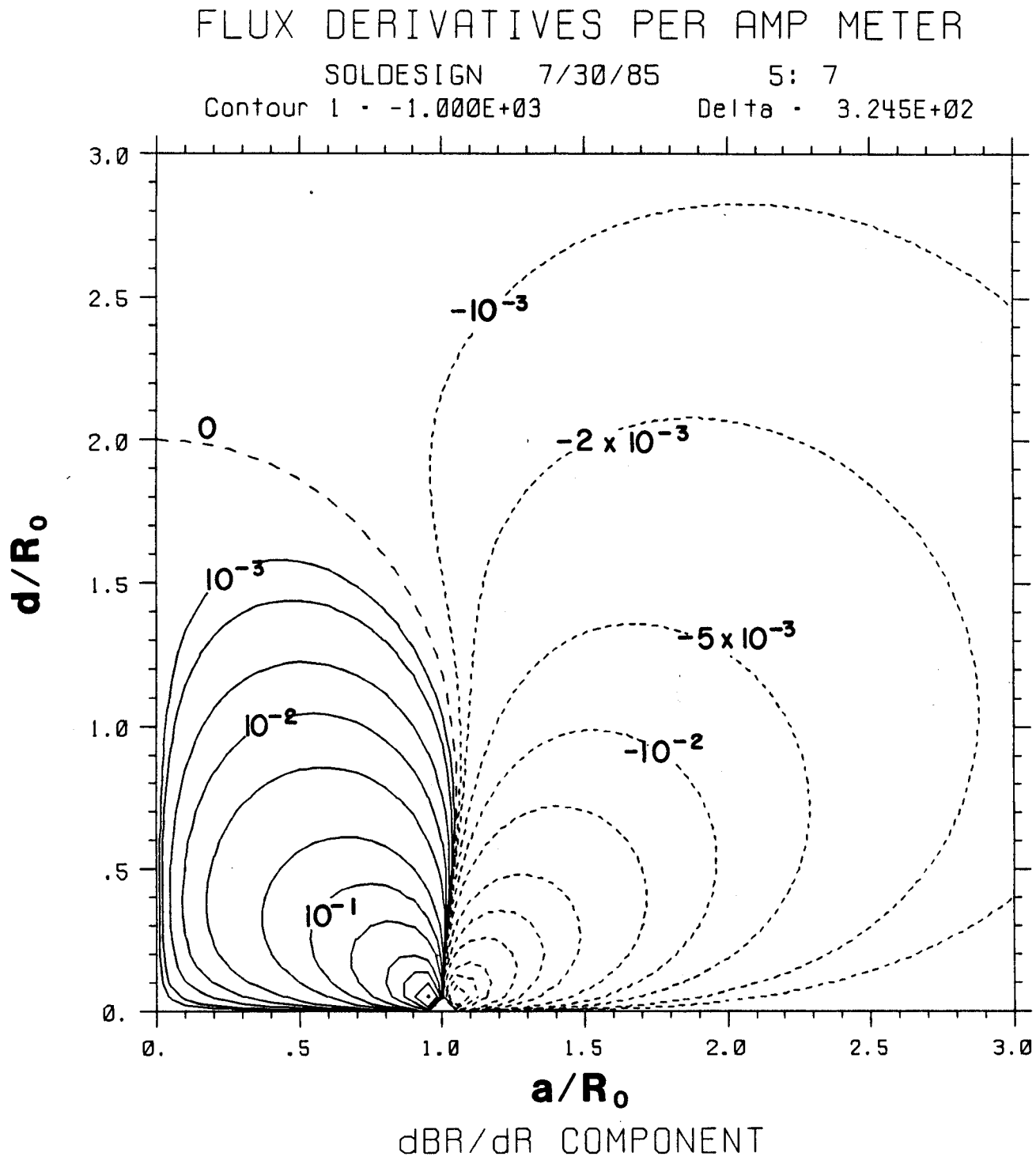

Fig. 21 - Normalized Contours of first derivative of B_r per ampere meter

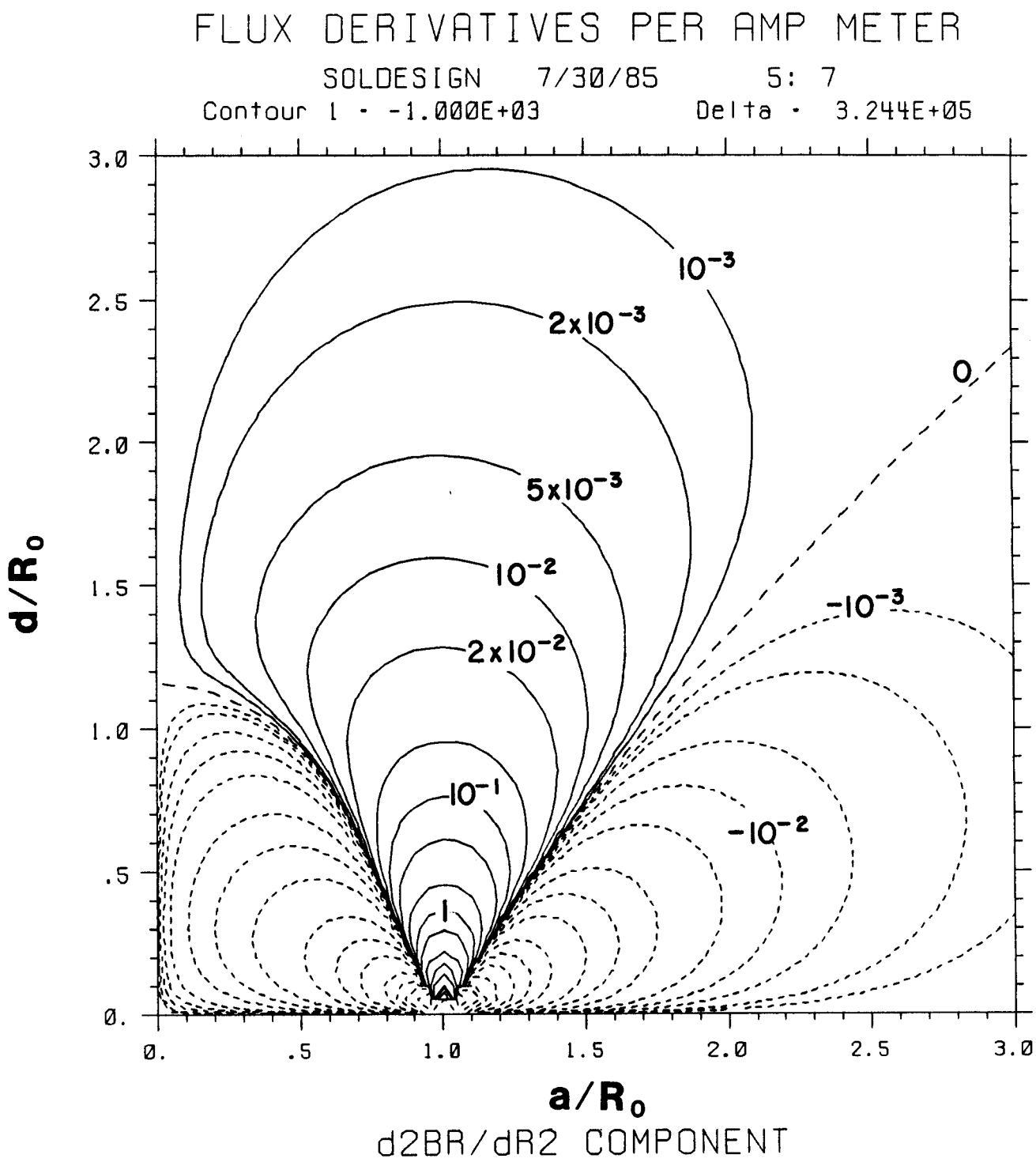

Fig. 22 - Normalized Contours of second derivative of B_r per ampere meter

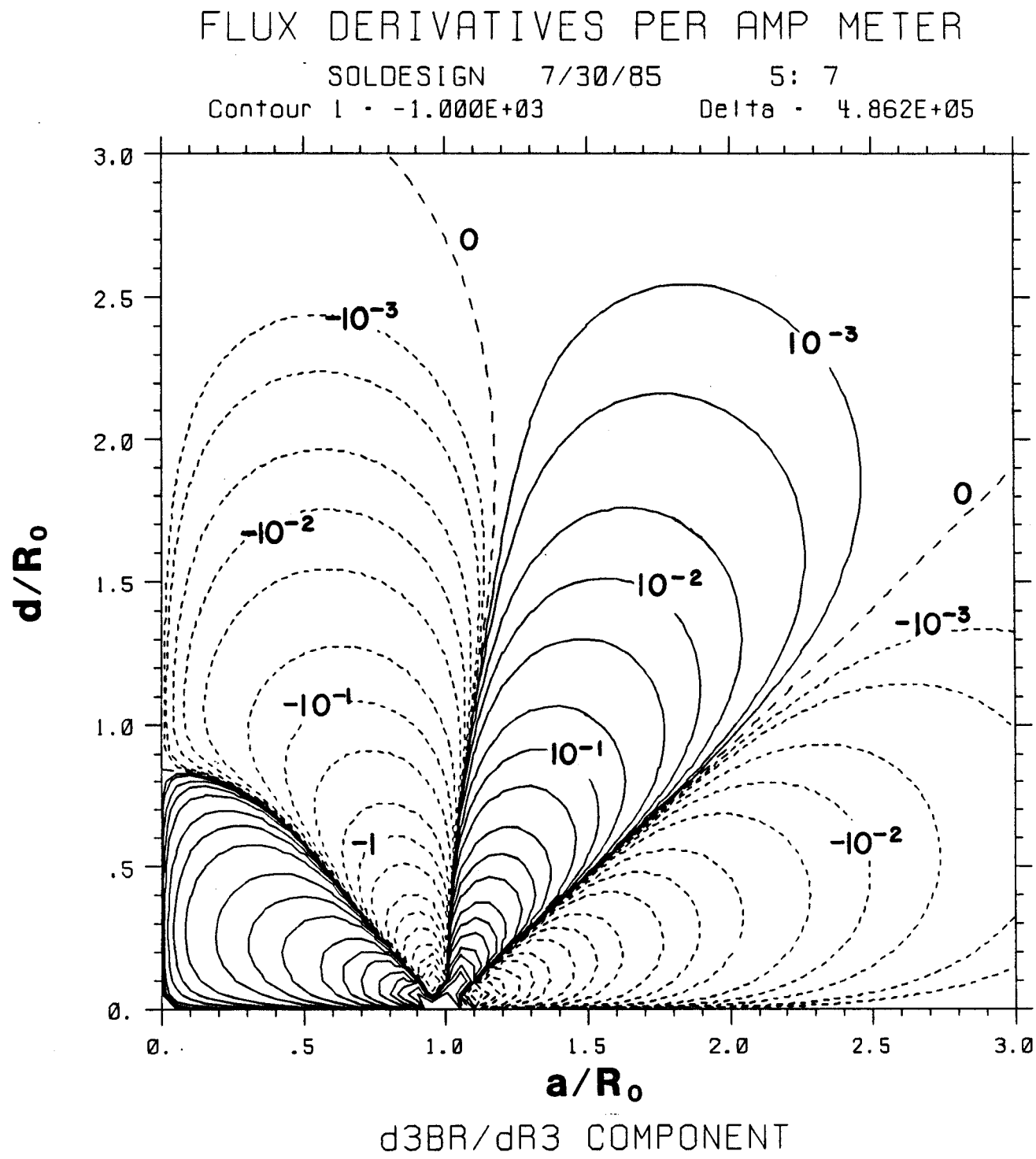

Fig. 23 - Normalized Contours of third derivative of B_r per ampere meter

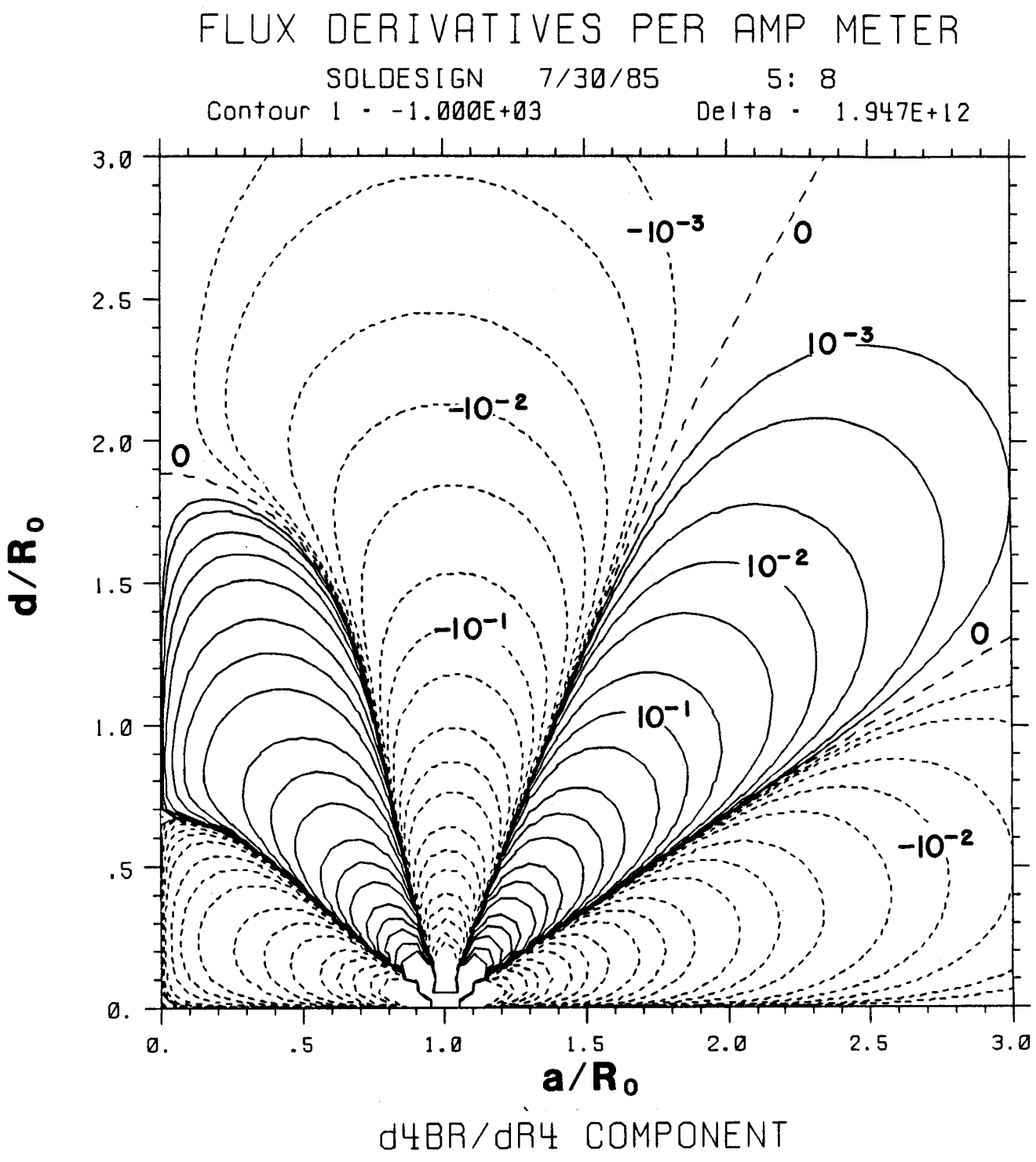

Fig. 24 - Normalized Contours of fourth derivative of B_r per ampere meter

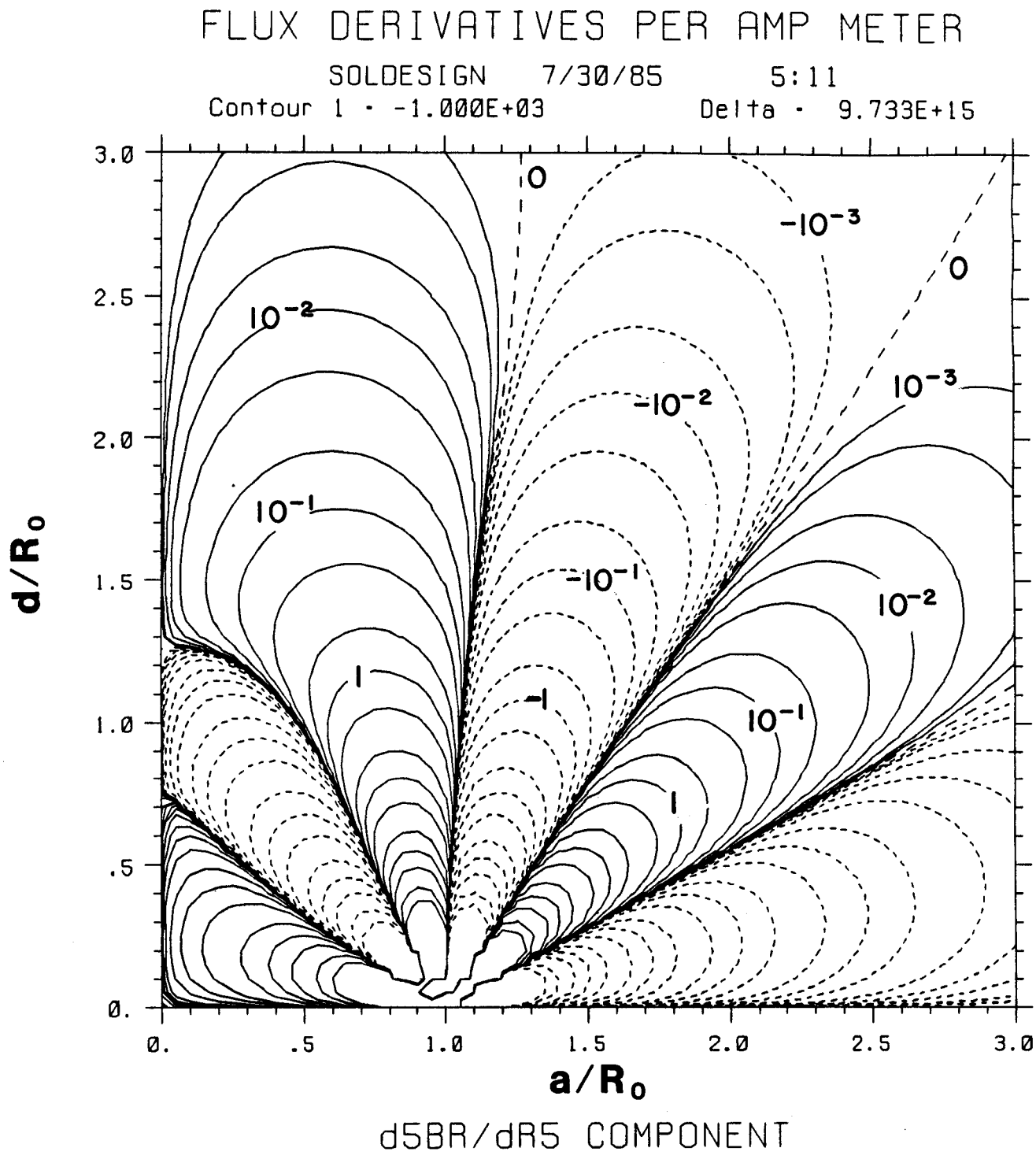

Fig. 25 - Normalized Contours of fifth derivative of B_r per ampere meter

In these charts, coils on a given contour will produce the same derivative at (1,0) for a given amount of (A•m).

EXAMPLE BASED ON AN IDEAL PF SET FOR A TOKAMAK

The currents required for plasma equilibrium computed using an equilibrium code described in [4] were determined for an ideal PF coil set (50 coils). Results are shown in Fig. 26 in which the size of each PF coil is proportional to the current it carries and shaded coils are carrying current into the page.

To illustrate the relative function of the different coils in producing the field derivative requirements, the currents were combined with their contour coefficients based on the magnitude of the functions, p_{nk}, in (2) and the coils were superimposed on selected effectiveness plots. An example is shown in Fig. 27 for the vertical field component and illustrates that the major part of this component is produced by the outermost coils. Figure 28 is for the second vertical field derivative which is effective in shaping the plasma. It shows that the inboard coils ideally create a significant portion of the total second order field derivative requirements for this case. Because of the change in sign of contours on the inboard side, the coil currents in this region also change sign so as to aid in the higher-order field production. This implies that the central ohmic heating coil stack (typically as high as $d/R_0 \sim 1$) in a combined OH and PF system should not be constrained to be driven by a single current source. This would negate the ability to provide the current reversal on the inboard side and force other coils to compensate with an increase in ampere-turns. The ideal height for the independent current region near the midplane of the OH stack will be related to the

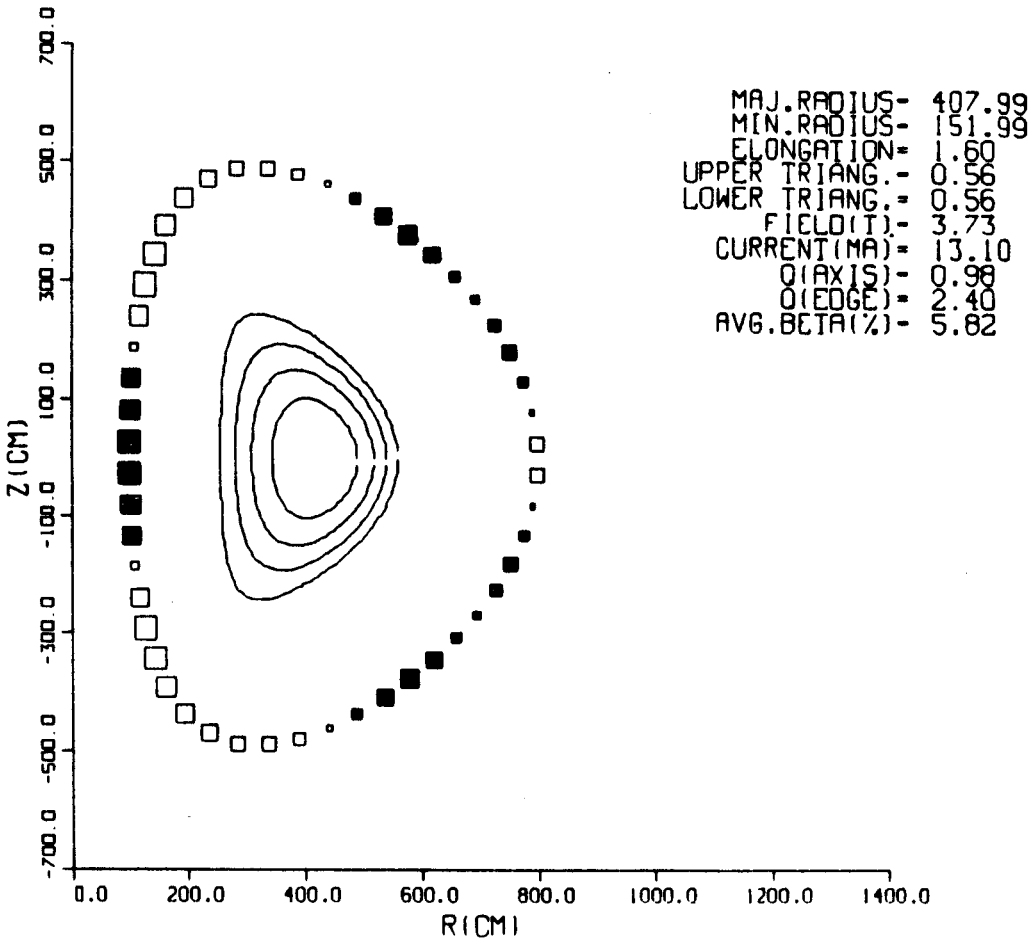

Fig. 26 - Equilibrium Code Output Plot for an Elongation of 1.6 and a Triangularity of 0.56

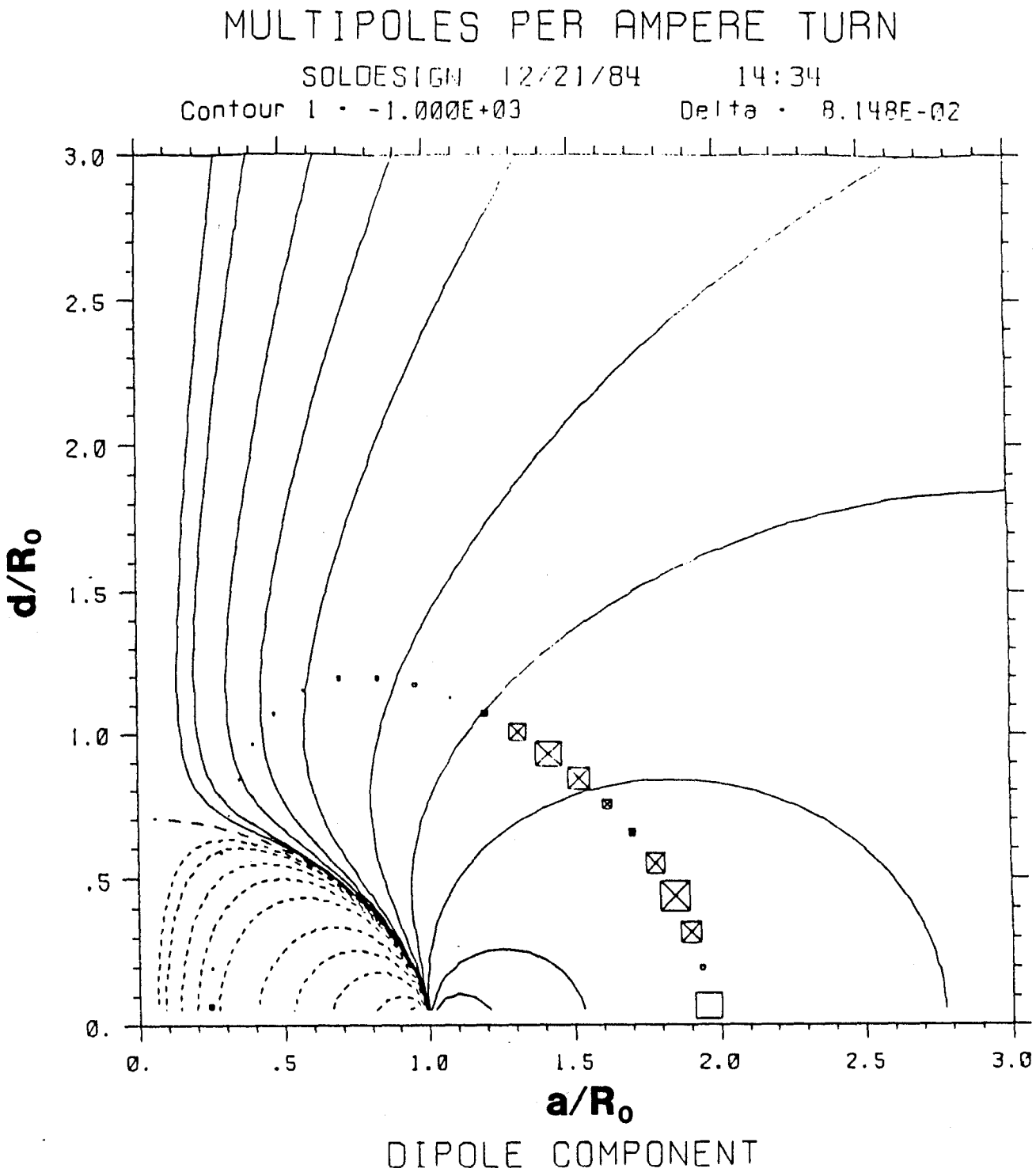

Fig. 27 - Relative Coil Contributions to the Vertical Field

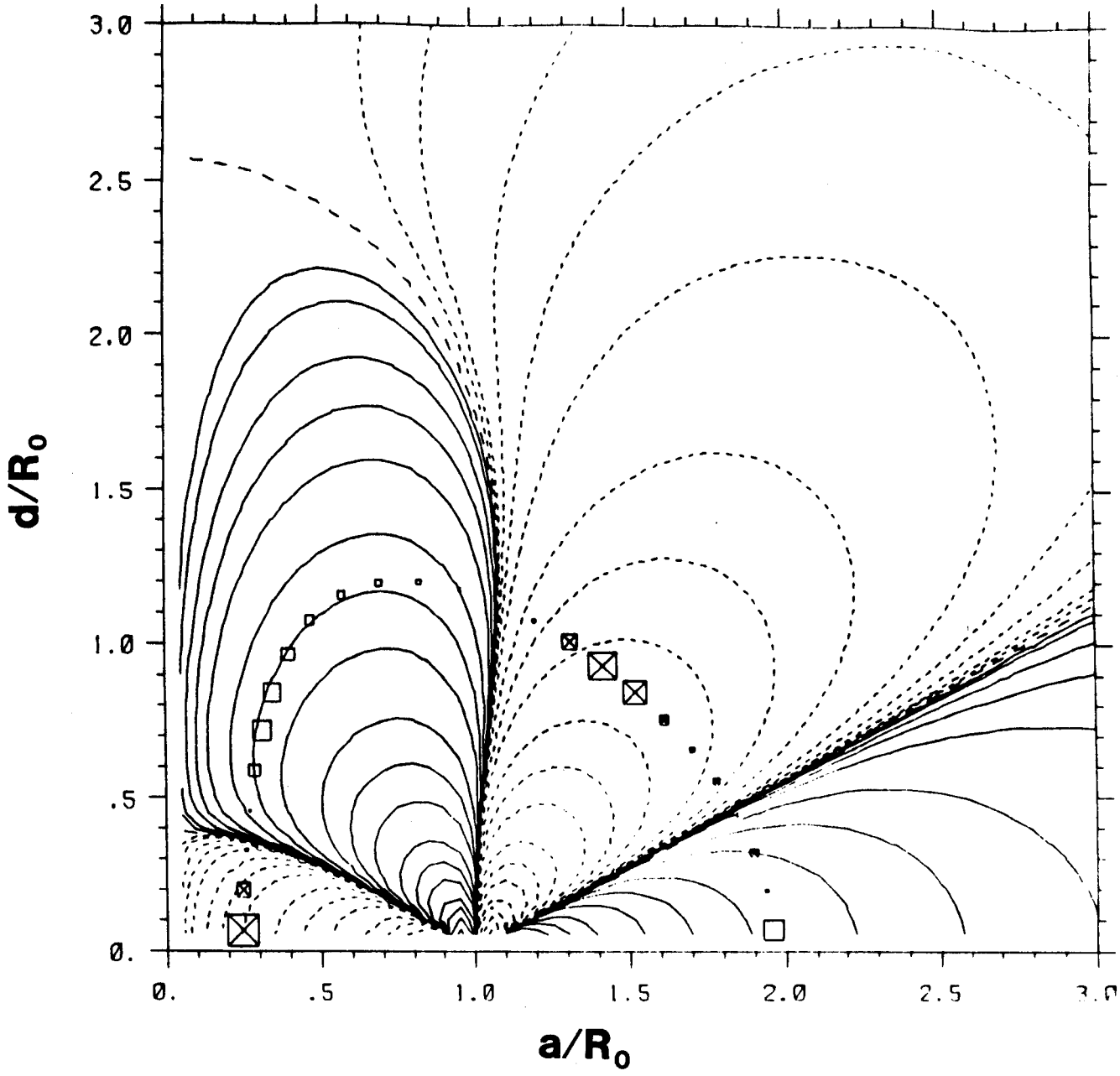

Fig. 28 - Relative Coil Contributions to the second derivative of B_z with respect to r for the case in Fig. 26

highest order dominant derivative required by the plasma shape because the effectiveness plots show that the height of the zero line on the inboard side decreases for derivatives of successively higher order. For plasmas of the type considered, the highest order dominant derivative is probably n = 3. Furthermore, the OH stack radius was typically at 0.35-0.4 of the major radius. The n = 3 plot shows that a reasonable height for the independent portion of the stack would be about 0.25 of the major radius since this will allow effective n = 3 production without being too close to the zero effectiveness line. In more highly shaped plasmas, higher orders will become important and the height of the independent stack near the midplane should probably be shorter.

CONCLUSIONS

General contour plots illustrate the effect of current loop location on the production of magnetic field components and their derivatives at an arbitrary point in normalized space. The plots give loci of coil positions which produce no contribution to specific derivatives and allow magnitudes to be determined for other cases by combining contour values with (2). They may be used to find loop locations or currents to create a desired field or derivative null at a given point.

For a tokamak, the contours show how minor changes in PF coil location can drastically affect the higher order field derivatives and, therefore, make PF coil location optimization difficult when the number of coils is small and significant shaping is required. They also imply the need for independent current control near the midplane of a typical OH coil stack.

REFERENCES

[1] W.R. Smythe - Static and Dynamic Electricity McGraw-Hill, New York, (1968).

[2] R.D. Pillsbury, Jr., R.J. Thome, J.M. Tarrh and W.R. Mann - "Poloidal Field Coil System Design Using a Field Expansion Technique" - Proc. 9th Inter. Conf. on Magnet Technology (MT-9), Zurich, September (1985).

[3] MACSYMA Reference Manual - The Mathlab Group, Lab for Computer Science, MIT, Cambridge, MA (1977).

[4] D.J. Strickler, J.B. Miller, K.E. Rothe and Y.K.M. Peng - "Equilibrium Modeling of the TFCX Poloidal Field Coil System" - ORNL/FEDC-83/10 (1983).

Appendix A
Field/Flux Derivatives Required for Coaxial Field Coil Design

A.1 Introduction

This section shows that matching a number of field derivatives at a point in space is sufficient to generate equivalent fields throughout a region in the vicinity of the point and to show which derivatives it is necessary to match. Cases which are symmetric and antisymmetric relative to the $z = z_0$ plane are considered separately since an unsymmetric case can always be treated by superposing a symmetric and an antisymmetric case. Because of the curl and divergence requirements on the field, there is some freedom in choosing the form of the Taylor series in terms of the form of the partial derivatives it is necessary to match. In this apppendix we choose to match partial derivatives of B_z with respect to radial position, r, for the symmetric situation and partial derivatives of B_r with respect to r for the antisymmetric case. The analytic form for these derivatives can be generated for a given current loop by taking successive derivatives of the vector potential or flux function for a circular current filament as mentioned earlier.

A.2 Symmetric Coil Distributions

In this case we are interested in coils which are coaxial and exist in pairs carrying currents which are symmetric relative to the $z = z_0$ plane. Because of the axial symmetry, the vector potential, $\bar{A}$ has a component only in the ϕ direction:

$$\bar{A}(r,z) = A(r,z)\bar{i}_\phi. \tag{1}$$

Note that $A(r,z)$ is related to the flux function ψ by the relation $\psi = 2\pi r A$ and that the following may therefore be carried out in terms of ψ if desired.

The vector potential can be determined in the vicinity of the point (r_0, z_0) by using a Taylor's series expansion as follows:

$$A(r_0+\Delta r, z_0+\Delta z) = \sum_{n=1}^{\infty} \frac{1}{(n-1)!}[(\Delta r\frac{\partial}{\partial r} + \Delta z\frac{\partial}{\partial z})^{n-1}A(r,z)]_{(r_0 z_0)} \tag{2}$$

where the expression in parentheses is to be expanded in a formal fashion by the binomial theorem and then applied as an operator to $A(r,z)$. After taking the indicated partial derivatives, the terms are to be evaluated at the point (r_0, z_0). Equation (2) can be rewritten as follows:

$$A(r_0+\Delta r, z_0+\Delta z) = A(r_0,z_0) + [(\Delta r\frac{\partial}{\partial r} + \Delta z\frac{\partial}{\partial z})A(r,z)]_{r_0 z_0}$$
$$+\frac{1}{2!}[((\Delta r)^2\frac{\partial^2}{\partial r^2} + 2\Delta r\Delta z\frac{\partial^2}{\partial r\partial z} + (\Delta z)^2\frac{\partial^2}{\partial z^2})A(r,z)]_{(r_0 z_0)}$$
$$+....+\frac{1}{(n-1)!}[(\Delta r\frac{\partial}{\partial r} + \Delta z\frac{\partial}{\partial z})^{n-1}A(r,z)]_{(r_0,z_0)} + R_n \quad (3)$$

where R_n, the remainder after n terms is given by:

$$R_n = \frac{1}{n!}[(\Delta r\frac{\partial}{\partial r} + \Delta z\frac{\partial}{\partial z})^n A(r,z)]_{(r_1,z_1)}, \quad (4)$$

where r_1 lies between r_0 and $r_0+\Delta r$ and z_1 lies between z_0 and $z_0+\Delta z$. Note that the magnitude of the error is in the $(n+1)$st term evaluated at some point (r_1, z_1) in the domain. The Taylor's series will converge to the value of $A(r_0+\Delta r, z_0+\Delta z)$ if, and only if:

$$\lim_{n\to\infty} R_n = 0. \quad (5)$$

If $A(r,z)$ is the vector potential due to the poloidal field, (r_0, z_0) is a point within the plasma cross section, and $(r_0+\Delta r, z_0+\Delta z)$ is a point within the plasma boundary, then the expansion can reconstruct the vector potential throughout that region (or, equivalently, the flux function or the field) with an error, R_n, if n terms are used.

The vector potential has been expanded using this technique to the seventh term (n=7). The derivatives of A were then expressed in terms of A, B_z, and the partial derivatives of B_z with respect to r by using the following relationships:

$$\bar{\nabla}\times\bar{A} = \bar{B} \quad (6)$$

$$\bar{\nabla}\cdot\bar{B} = 0 \quad (7)$$

$$\bar{\nabla}\times\bar{B} = \bar{0} \quad (8)$$

In terms of the components which exist in the configuration of Figure 1, equation (6) becomes

$$B_r = -\frac{\partial A}{\partial z}. \quad (9)$$

$$B_z = \frac{1}{r}\frac{\partial}{\partial r}(rA) = \frac{\partial A}{\partial r} + \frac{A}{r} \tag{10}$$

while equation (7) becomes

$$\frac{\partial B_z}{\partial z} = -\frac{1}{r}\frac{\partial}{\partial r}(rB_r) = -\frac{B_r}{r} - \frac{\partial B_r}{\partial r}. \tag{11}$$

and equation (8) becomes

$$\frac{\partial B_r}{\partial z} = \frac{\partial B_z}{\partial r}. \tag{12}$$

In addition, symmetry about the $z = z_0$ plane may be used to simplify, since this condition requires that

$$B_r = \frac{\partial B_r}{\partial r} = ... = \frac{\partial^m B_r}{\partial r^m} = 0 \tag{13}$$

when these terms are evaluated at $z = z_0$. Note that this does not limit the applicability or accuracy of the series for values of $z \neq z_0$ (i.e., for nonzero values of Δz). This is shown by equations (2) and (3), since the indicated terms are evaluated at the point (r_0, z_0) while finite values of Δz are used for $z \neq z_0$.

For the special case of $\Delta z = 0$, the final results are simplified in comparison to the general case of nonzero Δz. For $\Delta z = 0$, the vector potential can be expressed as

$$A(r_0 + \Delta r, z_0) = [1 + \frac{\Delta r}{r_0}]^{-1}\{A - \sum_{n=1}^{\infty} \frac{\partial^{n-1} B_z}{\partial r^{n-1}}[\frac{(\Delta r)^n}{n!}][1 + (\frac{n}{n+1})(\frac{\Delta r}{r_0})]\} \tag{14}$$

or as

$$A(r_0 + \Delta r, z_0) = [1 + \frac{\Delta r}{r_0}]^{-1}\{A + \sum_{n=1}^{\infty} \frac{(\Delta r)^n}{n!}\frac{\partial^{n-1} B_z}{\partial r^{n-1}} g_n(\Delta r/r_0)\} \tag{15}$$

where

$$g_n(\Delta r/r_0) = [1 + (\frac{n}{n+1})(\frac{\Delta r}{r_0})]$$

The functions g_n are dependent only on the location of the point of interest and not on the location of the field source which produces the derivatives. Again, A, B_z, and the partial derivatives of B_z are all to be evaluated at $(r, z) = (r_0, z_0)$.

When the general case of $\Delta z \neq 0$ is considered, all of the terms g_n which multiply the partial derivative terms of equation (15) (beginning with the first partial derivative term, i.e.,$n = 2$) contain additional factors which depend on $\Delta z/\Delta r$ as well as $\Delta r/\Delta r_0$. One may therefore express the vector potential in the neighborhood of (r_0, z_0) simply in

terms of A, B_z,and $\partial^m B_z/\partial r^m$ all evaluated at (r_0, z_0) plus functions $f_n(\Delta r/r_0, \Delta z/\Delta r)$ which again depend only on the location of the point of interest. In functional form,

$$A(r_0 + \Delta r, z_0 + \Delta z) = [1 + \frac{\Delta r}{r_0}]^{-1}\{A + \sum_{n=1}^{\infty} \frac{(\Delta r)^n}{n!} \frac{\partial^{n-1} B_z}{\partial r^{n-1}} f_n(\frac{\Delta r}{r_0}, \frac{\Delta z}{\Delta r})\}. \qquad (16)$$

Note that the extremes of the variables of the f_n functions are equivalent to significant geometric parameters in a tokamak. For example, if r_0 is the major radius, then since the extreme value of Δr is the plasma minor radius, the ratio $\Delta r/r_0$ in the inverse aspect ratio. In addition, since the extreme value of Δz is the half height of the plasma, then $\Delta z/\Delta r$ is the elongation. In equation (16), the other derivative terms (such as $\partial^m B_r/\partial z^m$, for example) are not needed due to the field relationships and symmetry given by equations (6) through (13).

If the flux function ψ is preferred, then equation (16) can be rewritten as

$$\psi(r_0 + \Delta r, z_0 + \Delta z) = \psi(r_0, z_0) + (2\pi r_0) \sum_{n=1}^{\infty} \frac{(\Delta r)^n}{n!} \frac{\partial^{n-1} B_z}{\partial r^{n-1}} f_n(\frac{\Delta r}{r_0}, \frac{\Delta z}{\Delta r}). \qquad (17)$$

Equations (16) and (17) show that two different PF coil sets will produce the same symmetric field throughout the plasma region provided they produce the same vector potential or flux function at (r_0, z_0) and provided they have the same values for the B_z field derivatives with respect to r at that point. The number of terms which should be included in the matching process is dependent on the level of shaping required. The error which is introduced by truncation or by not exactly matching individual poles requires investigation.

3.0 Antisymmetric Coil Distributions

An antisymmetric coil pair has coils symmetrically located relative to the $z = z_0$ plane, but has equal and opposite currents in each coil. In this situation B_z and its derivatives with respect to r will be zero in the $z = z_0$ plane. The expanded formulation for the vector potential is still given by equations (1) through (5).

The field constraints imposed by $\bar{\nabla} \times \bar{A} = \bar{B}, \bar{\nabla} \cdot \bar{B} = 0$, and $\bar{\nabla} \times \bar{B} = \bar{0}$ remain as given in equations (9) through (12). However, the symmetry condition now yields the following at $z = z_0$:

$$\frac{\partial B_r}{\partial z} = \frac{\partial B_z}{\partial r} = 0. \qquad (18)$$

In addition,

$$B_z = 0 \Rightarrow \frac{\partial A}{\partial r} = \frac{-A}{r} = 0. \tag{19}$$

If a similar process of Taylor series expansion, simplification, and collection of terms is carried out for this antisymmetric case, the vector potential and flux function can be shown to be given by:

$$A(r_0 + \Delta r, z_0 + \Delta z) = (1 + \frac{\Delta r}{r_0})^{-1} \sum_{n=1}^{\infty} \frac{(\Delta r)^n}{(n-1)!} \frac{\partial^{n-1} B_r}{\partial r^{n-1}} h_n(\frac{\Delta r}{r_0}, \frac{\Delta z}{\Delta r}) \tag{20}$$

$$\psi(r_0 + \Delta r, z_0 + \Delta z) = (2\pi r_0) \sum_{n=1}^{\infty} \frac{(\Delta r)^n}{(n-1)!} \frac{\partial^{n-1} B_r}{\partial r^{n-1}} h_n(\frac{\Delta r}{r_0}, \frac{\Delta z}{\Delta r}). \tag{21}$$

Equations (20) and (21) show that two different coil sets will produce the same antisymmetric field throughout the plasma region provided they produce the same vector potential or flux function at r_0, z_0 and provided they have the same values for the B_r field derivatives with respect to r at that point. The number of terms which should be included in the matching process is dependent on the level of shaping required. The error which is introduced by truncation or by not exactly matching individual poles for this case requires investigation.